

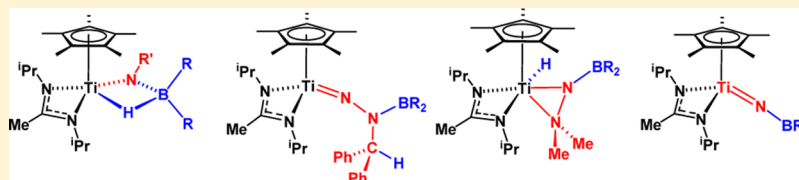
Reactions of Titanium Imides and Hydrazides with Boranes

Simona Mellino,[†] Laura C. Stevenson,[†] Eric Clot,^{*,‡,§} and Philip Mountford^{*,†,§}

[†]Chemistry Research Laboratory, Department of Chemistry, University of Oxford, Mansfield Road, Oxford OX1 3TA, U.K.

[‡]Institut Charles Gerhardt Montpellier, UMR 5253 CNRS-UM-ENSCM, Université de Montpellier, cc 1501, Place Eugène Bataillon, F-34095 Montpellier Cedex 5, France

S Supporting Information



ABSTRACT: We report the first reactions of titanium imido, alkylidene hydrazido, and dimethylhydrazido compounds with the boranes H₂B^{Tex}, 9-BBN, HBAr^F₂, and HBPin (Tex = *tert*-hexyl; Ar^F = C₆F₅). Reactions of Cp^{*}Ti{MeC(NⁱPr)₂} (NTol) with H₂B^{Tex}, 9-BBN, or HBAr^F₂ resulted in the hydride-bridged adducts Cp^{*}Ti{MeC(NⁱPr)₂}{N(Tol)HBRR'} without B–H bond cleavage. Cp^{*}Ti{MeC(NⁱPr)₂} (NNCPh₂) (**4**) reacted with HBAr^F₂ via a sequence of steps involving adducts at the β- and then α-nitrogen of the NNCPh₂ ligand, before slow 1,2-addition of B–H across the N=CPh₂ double bond of **4**, forming Cp^{*}Ti{MeC(NⁱPr)₂}{NN(BAr^F₂)CHPh₂} (**17**). The other boranes reacted immediately with **4** to form homologues of **17**. These products are the first examples of borylhydrazido(2-) complexes. Reaction of Cp^{*}Ti{MeC(NⁱPr)₂} (NNMe₂) (**2**) with HBAr^F₂ gave the hydride-bridged adduct Cp^{*}Ti{MeC(NⁱPr)₂}{N(NMe₂)HBAr^F₂}, whereas with HBPin B–H bond cleavage occurred to form the borylhydrazido(1-)-hydride Cp^{*}Ti{MeC(NⁱPr)₂} (H){N(BPin)NMe₂}. Finally, reaction of **2** with 9-BBN dimer resulted in H₂ elimination and formation of Me₂NBC₈H₁₄ and Cp^{*}Ti{MeC(NⁱPr)₂} (NBC₈H₁₄), a rare example of a borylimido compound.

INTRODUCTION

A series of reviews and recent papers have charted the remarkable developments in Group 4 imido (L)M(NR),¹ hydrazido (L)M(NNR₂),² and alkylidene hydrazido/diazoalkane (L)M(NNCR₂)³ compounds over the last ca. 25 years (L = supporting ligand set; R = H or hydrocarbyl). Other classes of Group 4 imido-type compounds featuring heteroatom substituents have also been recently reported, namely the titanium *tert*-butoxyimides (L)Ti(NO^tBu)⁴ and borylimides (L)Ti(NBR₂).⁵ In general, the dominant feature of these compounds is their addition or insertion reactions with unsaturated compounds at the M–N_α multiple bond itself (best described as a σ²π⁴ triple bond). For certain hydrazido,⁶ alkylidene hydrazido,^{3c} and *tert*-butoxyimido^{4a,c} compounds, reductive cleavage of the N_α–N_β or N_α–O_β bond can occur with reducing substrates such as CO, isonitriles, and alkynes. Less commonly, dating from Bergman and Wolczanski's first reports on these compounds,⁷ Group 4 imides can also activate the C–H bonds of organic substrates, and also the H–H bond of H₂. As documented in the reviews,^{1a–c,e,g} many significant advances regarding these aspects have been achieved.^{3d,8}

In contrast, Si–H and, especially, B–H bond activation reactions of Group 4 imido and hydrazido-type compounds with silanes and boranes are still poorly developed, although they are better known for transition metal–heteroatom multiple bonds in general.⁹ There are no reported Si–H additions to Group 4 imides. In related chemistry, Si–H 1,2-

addition to the Ti–S bond of Cp₂Ti(S)(py) and to a strained tantalum imide was reported some time ago.^{9c,d} Very recently a scandium imide was shown to activate Si–H bonds by 1,2-addition to Sc–N_α, albeit in a reversible equilibrium.^{9e}

The situation with hydrazides and alkylidene hydrazides is better established, at least for titanium. Andersen and Bergman found that Cp₂Ti(η²-NNCHTol) reacted with PhSiH₃ or Ph₂SiH₂ by 1,2-addition to Ti–N_α forming alkylidene hydrazide(1-)-hydride products, **1**, as illustrated in Figure 1.^{3c} We subsequently reported that the dimethylhydrazide Cp^{*}Ti{MeC(NⁱPr)₂} (NNMe₂) (**2**) forms analogous 1,2-addition products, **3** (Figure 1), with primary aryl silanes ArSiH₃ or BuSiH₃ in a reversible equilibrium.¹⁰ No reaction occurred with the diphenylhydrazido or imido counterparts of **2**. DFT calculations found that, without additional coordination of the β-NMe₂ group in **3**, 1,2-addition to Ti–N_α was thermodynamically unfavorable. The alkylidene hydrazide analogue of **2**, Cp^{*}Ti{MeC(NⁱPr)₂} (NNCPh₂) (**4**), also reacted with ArSiH₃ or Ph₂SiH₂, forming N,N'-disubstituted hydrazide(2-) products **5**, featuring net 1,3 Si–H bond addition across the N=N=CPh₂ moiety of **4**.^{3c} Mechanistically, this proceeds via 1,2-addition of Si–H to Ti–N_α to give a hydrazide(1-)-hydride intermediate, analogous to **1** and **3**,

Received: June 23, 2017

Published: August 22, 2017



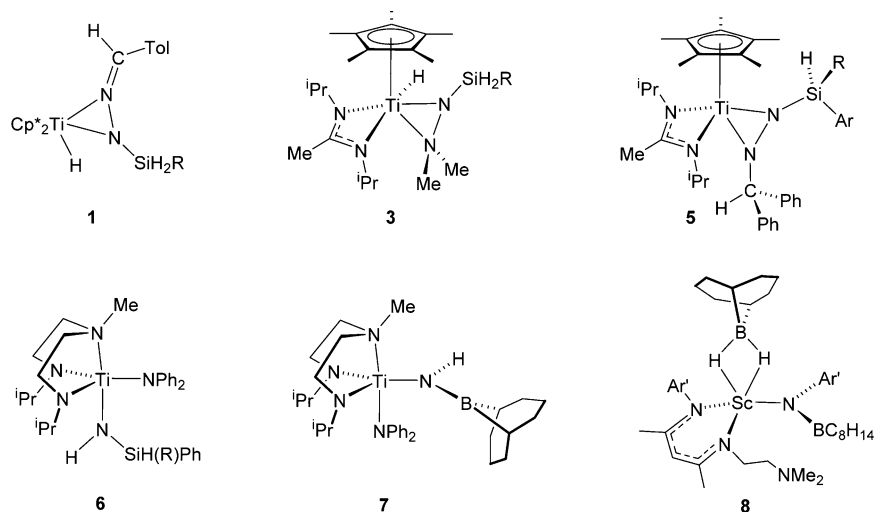


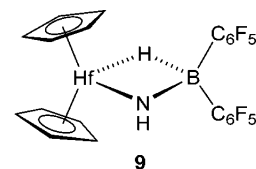
Figure 1. Examples of products of Si–H or B–H bond activation with imido and hydrazido compounds ($\text{Ar}' = 2,6\text{-C}_6\text{H}_3\text{iPr}_2$).^{3c,e,5b,9f,10}

followed by hydride migration to the electrophilic $\text{N}_\beta\text{CPh}_2$ carbon.

Very recently we also reported the reductive $\text{N}_\alpha\text{--N}_\beta$ bond cleavage reactions of $\text{Ti}(\text{N}_2\text{N}^{\text{Me}})(\text{NNPh}_2)(\text{py})$ with PhSiH_3 and Ph_2SiH_2 .^{5b} DFT and kinetic studies found that this reaction proceeds via concerted Si–H bond addition across the Ti– N_α bond to again form a hydrazide(1)-hydride intermediate (cf. 1 and 3). Subsequent hydride migration to the N_α atom of the so-formed $\eta^2\text{-N}(\text{SiH}_2\text{R})\text{NPh}_2$ ligand is coupled with $\text{N}_\alpha\text{--N}_\beta$ bond cleavage, forming 6 (Figure 1). Furthermore, reaction of $\text{Ti}(\text{N}_2\text{N}^{\text{Me}})(\text{NNPh}_2)(\text{py})$ with 9-BBN ($[(\mu\text{-H})\text{BC}_8\text{H}_{14}]_2$) formed the borylamide counterpart 7, and DFT and kinetic studies established an analogous mechanism to that for 6.^{5b,11} A homologous compound to 6 was formed using HBMe_2 ($\text{Mes} = 2,4,6\text{-C}_6\text{H}_2\text{Me}_3$), but with pinacol borane (HBPIn) or Piers' borane¹² (HAr^{F_2} , $\text{Ar}^{\text{F}} = \text{C}_6\text{F}_5$) mixtures or undesired products of ligand transmetalation were obtained.¹¹

The $\text{N}_\alpha\text{--N}_\beta$ bond cleavage processes leading to 6 and 7 were the first of their type with silanes or boranes. More generally, the reactions of $\text{Ti}(\text{N}_2\text{N}^{\text{Me}})(\text{NNPh}_2)(\text{py})$ with HBR_2 were the first B–H activation reactions reported for any metal hydrazide. Furthermore, the first B–H activation reaction of an imide was described only recently by Chen for a scandium compound reacting with 9-BBN, forming 8 (Figure 1).^{9f} Subsequently Walter et al. reported the first B–H 1,2-addition reaction of an actinide imide for $(\eta\text{-C}_5\text{H}_2\text{Bu}_3)_2\text{Th}(\text{NTol})$ ($\text{Tol} = 4\text{-C}_6\text{H}_4\text{Me}$) with 9-BBN.¹³ No well-defined reactions of Group 4 imides with the B–H bonds of boranes have so far been reported. However, Lancaster recently showed that reaction of Cp_2HfCl_2 with 2 equiv of the lithiated borylamide $\text{LiNH}_2\text{BAr}^{\text{F}_2}$ formed $\text{Cp}_2\text{Hf}\{\text{N}(\text{H})\text{BAr}^{\text{F}_2}\}$ (9) as one component of a mixture, with the overall elimination of $\text{H}_3\text{NBAr}^{\text{F}_2}$ and LiCl .¹⁴ Although 9 appears formally to be the product of the 1,2-addition of HBAr^{F_2} to the Hf– N_α bond of $\text{Cp}_2\text{Hf}(\text{NH})$ (not known as an isolated species), the mechanism of its formation is unclear and probably proceeds via an amidohydroborate intermediate that is subsequently dehydrohalogenated by additional $\text{LiNH}_2\text{BAr}^{\text{F}_2}$.

Overall, the B–H bond activation reactions of Group 4 imides and hydrazides/alkylidene hydrazides have not been developed in any detail, although there are encouraging and interesting precedents as outlined above. In this contribution we report the reactions of titanium compounds of this type



with different types of primary and secondary boranes. A part of this work has been reported in a preliminary communication.^{5b}

RESULTS AND DISCUSSION

As described in the Introduction, we found previously that titanium half-sandwich amidinate compounds of the type $\text{Cp}^*\text{Ti}\{\text{MeC}(\text{N}^{\text{iPr}})_2\}(\text{NR})$ ($\text{R} = \text{hydrocarbyl}$, NCPH_2 or NR'_2) provided good starting points for developing Si–H bond activation chemistry of imido and hydrazido compounds.^{3e,10} We therefore used this class of compound for our current study with boranes. Preliminary screening with several borane types (*vide infra*) established that the tolylimide $\text{Cp}^*\text{Ti}\{\text{MeC}(\text{N}^{\text{iPr}})_2\}(\text{NTol})$ (10), alkylidene hydrazide $\text{Cp}^*\text{Ti}\{\text{MeC}(\text{N}^{\text{iPr}})_2\}(\text{NNCPH}_2)$ (4), and dimethylhydrazide $\text{Cp}^*\text{Ti}\{\text{MeC}(\text{N}^{\text{iPr}})_2\}(\text{NNMe}_2)$ (2) (Figure 2) gave the best outcomes in terms of reactivity and product isolation. For example, the *tert*-butylimide $\text{Cp}^*\text{Ti}\{\text{MeC}(\text{N}^{\text{iPr}})_2\}(\text{N}^{\text{iBu}})$ did not react with boranes, and the diphenylhydrazide $\text{Cp}^*\text{Ti}\{\text{MeC}(\text{N}^{\text{iPr}})_2\}(\text{NNPh}_2)$ reacted only with 9-BBN, under forcing conditions as discussed later on. In a similar way, we screened a number of

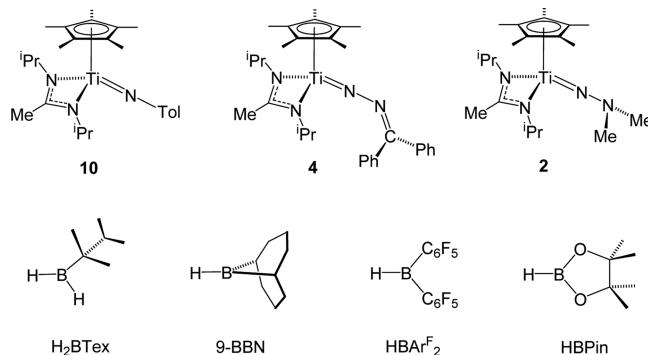
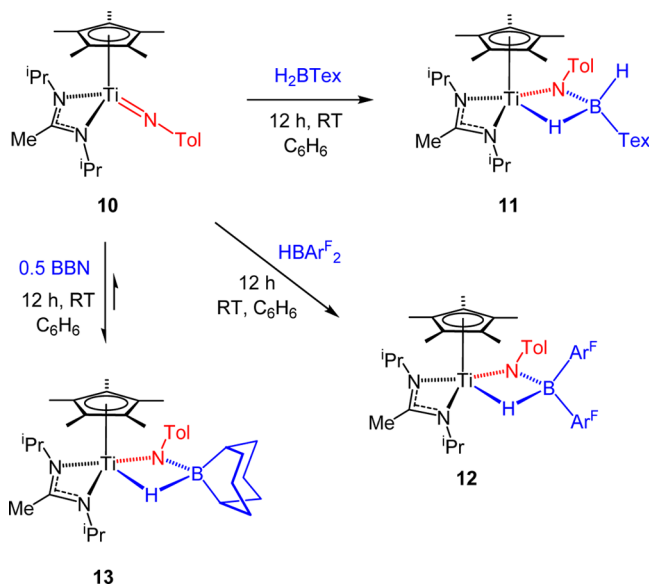


Figure 2. Principal titanium compounds and hydroboranes (shown in their monomeric form) used in this study.

hydroboranes possessing different substitution patterns at boron. The successful candidate boranes carried forward from these trials are listed in Figure 2 and represent primary (H_2BTex , $\text{Tex} = \text{tert-hexyl}$)¹⁵ and secondary boranes. Among the latter set there are electron-poor (HBAr^{F}_2)¹², dialkyl (9-BBN), and electron-rich (HBPin) homologues. Among other boranes assessed were HBCy_2 ,¹⁶ HBMe_2 ,¹⁷ $\text{HB}(\text{NAr}'\text{CH})_2$,¹⁸ $\text{HB}(\text{N}^i\text{PrCH}_2)_2$,¹⁹ and HBCat ($\text{Cat} = 1,2\text{-O}_2\text{C}_6\text{H}_4$). These either gave nonisolable equilibrium mixtures, poorly defined products, or no reaction at all. In addition we also carried out reactions of the *tert*-butoxyimide $\text{Cp}^*\text{Ti}\{\text{MeC}(\text{N}^i\text{Pr})_2\}\text{-(NO}^t\text{Bu)}$ (known to undergo Ti-N_α addition or $\text{N}_\alpha\text{-O}_\beta$ cleavage reactions with unsaturated substrates⁴) with boranes and silanes. Unfortunately complexes of unknown mixtures were invariably formed in this case.

Reactions of $\text{Cp}^*\text{Ti}\{\text{MeC}(\text{N}^i\text{Pr})_2\}(\text{NTol})$ (10) with boranes. Initial NMR tube scale reactions of 10 with H_2BTex or HBAr^{F}_2 proceeded cleanly to completion over several hours to form $\text{Cp}^*\text{Ti}\{\text{MeC}(\text{N}^i\text{Pr})_2\}\{\text{N}(\text{Tol})\text{H}_2\text{BTex}\}$ (11) and $\text{Cp}^*\text{Ti}\{\text{MeC}(\text{N}^i\text{Pr})_2\}\{\text{N}(\text{Tol})\text{HBAr}^{\text{F}}_2\}$ (12) as summarized in Scheme 1. On the preparative scale, the new compounds

Scheme 1. Reactions of $\text{Cp}^*\text{Ti}\{\text{MeC}(\text{N}^i\text{Pr})_2\}(\text{NTol})$ (10) with Boranes (shown in their monomeric forms)



were isolated as yellow/brown powders in 60–75% yield after workup. The reaction of 10 with 9-BBN is discussed below, and no reaction occurred between 10 and HBPin.

The NMR spectra of 11 and 12 are consistent with the structures illustrated, and in particular their ^{11}B NMR chemical shifts of 1.5 and -7.7 ppm, respectively, are consistent with four-coordinate boron environments.²⁰ The infrared spectrum of 11 showed two $\nu(\text{B-H})$ bands as expected: one at 2327 cm^{-1} for the terminal B-H unit and one at 1908 cm^{-1} for the B-H bridging to titanium. For 12, this $\nu(\text{B-H})_b$ mode appears at a slightly higher frequency (1939 cm^{-1}) suggesting a slightly stronger interaction of the hydride with boron as compared to 11. Diffraction-quality crystals of 11 and 12 were grown from pentane. The solid state structures are shown in Figure 3; selected bond lengths and angles are listed in Table 1.

Compounds 11 and 12 each have 4-legged piano stool geometries. The $\text{Ti-N}(2,3)$ and Ti-Cp^* distances and

associated angles for the supporting ligand sets are comparable and within the expected ranges.²¹ The $\text{Ti}(1)\text{-N}(1)$ bond distances are very similar, and their average value of $1.877(1)\text{ \AA}$ is significantly lengthened compared to the typical values of $1.71\text{--}1.73\text{ \AA}$ found in analogues of 10 (the X-ray structure of 10 itself has not been determined)²² but somewhat shorter than the Ti-N distances typically found for titanium amido compounds in general (*ca.* $1.93\text{--}2.03\text{ \AA}$) and for $[2 + 2]$ cycloaddition products of titanium arylimides (*ca.* $1.94\text{--}2.04\text{ \AA}$).²¹ The $\text{N}(1)\text{-B}(1)$ distances (av. $1.544(2)\text{ \AA}$) in 11 and 12 are also comparable to each other and are in the range found for amidohydroborate complexes ($[\kappa^2\text{-H}_2\text{RBNR}'_2]^-$ ligands, typically *ca.* $1.52\text{--}1.56\text{ \AA}$), known for a range of metals.²¹ The $\text{N}(1)\text{-B}(1)$ distance of $1.5426(14)\text{ \AA}$ in 12 can also be compared with the corresponding value of $1.509(10)\text{ \AA}$ in Lancaster's $\text{Cp}_2\text{Hf}\{\text{N}(\text{H})\text{HBAr}^{\text{F}}_2\}$ (9). The longer distance in 12 is attributed to the increased steric pressure at N_α from the tolyl group. The ^{11}B NMR chemical shift of -7.7 ppm in 12 is less negative than in 9 ($\delta = -27.5$ ppm), consistent with a better developed N-B interaction in the latter case.

The B-bound H atoms in 11 and 12 were located in the respective Fourier difference maps and were positionally and isotropically refined. The $\text{Ti}(1)\text{-H}(1)$ distances of $1.914(13)$ and $2.009(13)$ are significantly longer than in terminal titanium(+4) hydrides in general (av. 1.66 \AA , range $1.55\text{--}1.85\text{ \AA}$ for nine compounds in the current Cambridge Crystallographic Database²¹), and in the more closely related compounds 3 (Figure 1, av. 1.61 \AA). The $\text{Ti}(1)\text{-H}(1)$ bond in 12 is longer ($\Delta(\text{Ti-H}) = 0.10(2)\text{ \AA}$) than in 11, and its $\text{B}(1)\text{-H}(1)$ is apparently shorter ($\Delta = 0.05(2)\text{ \AA}$). This is attributed to the electron-withdrawing nature of the C_6F_5 groups, which render the boron atom more Lewis acidic, despite the greater steric crowding in 12. The DFT structures (B3PW91 including corrections for dispersion and solvent effects, see the Experimental Section) have been calculated for 11 and 12. The DFT structure of 11 is shown in Figure 4, and key selected distances for 11 and 12 are given in the caption. The DFT structures confirm the key features of the X-ray structures and are discussed in further detail below.

Reaction of $\text{Cp}^*\text{Ti}\{\text{MeC}(\text{N}^i\text{Pr})_2\}(\text{NTol})$ (10) with 0.5 equiv of 9-BBN dimer formed $\text{Cp}^*\text{Ti}\{\text{MeC}(\text{N}^i\text{Pr})_2\}\{\text{N}(\text{Tol})\text{-HBC}_8\text{H}_{14}\}$ (13) which was isolated as a viscous oil on workup. The NMR and IR spectra of 13 are consistent with the structure shown in Scheme 1 which is analogous to those of 11 and 12. The ^{11}B NMR resonance in 13 appears at 10.4 ppm, consistent with a four-coordinate boron²⁰ (note that the ^{11}B resonance in 7 (Figure 1) appears at 54.4 ppm for three-coordinate boron^{5b}). The IR spectrum of 13 features a $\nu(\text{B-H})_t$ band at 1651 cm^{-1} . Even though this value is comparatively low, it is nonetheless at a significantly higher frequency than for $\nu(\text{Ti-H})$ in the silylhydrazide(1-)-hydride compounds 3 ($1565\text{--}1585\text{ cm}^{-1}$),^{10a} suggesting that an analogous borylamide-hydride product $\text{Cp}^*\text{Ti}\{\text{MeC}(\text{N}^i\text{Pr})_2\}(\text{H})\{\text{N}(\text{Tol})\text{-BC}_8\text{H}_{14}\}$ has not been formed.

The DFT structure of 13 is shown in Figure 4 together with selected distances. The Ti-H_b and B-H_b distances are significantly shorter and longer, respectively, than in 11 and 12, showing a better-developed hydride transfer from boron to titanium, attributed to the more electron-releasing alkyl substituents in the case of 13. The computed $\nu(\text{B-H})_b$ frequencies are 1891 cm^{-1} , 1939 cm^{-1} , and 1755 cm^{-1} for 11, 12, and 13, respectively, in agreement with experimental trends. The calculated ^{11}B NMR shifts are 2.0, -6.7 , and 8.0

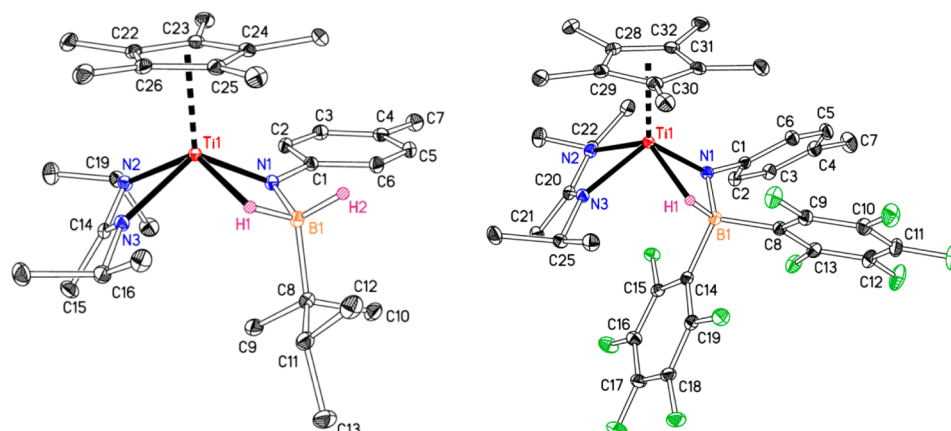


Figure 3. Displacement ellipsoid plots (25% probability) of $\text{Cp}^*\text{Ti}\{\text{MeC}(\text{N}^i\text{Pr}_2)_2\}\{\text{N}(\text{Tol})\text{H}_2\text{BTeX}\}$ (**11**, left) and $\text{Cp}^*\text{Ti}\{\text{MeC}(\text{N}^i\text{Pr}_2)_2\}\{\text{N}(\text{Tol})\text{HBCAr}^{\text{F}}_2\}$ (**12**, right). C-bound H atoms are omitted for clarity. Remaining H atoms are drawn as spheres of an arbitrary radius.

Table 1. Selected Bond Distances (Å) and Angles (deg) for $\text{Cp}^*\text{Ti}\{\text{MeC}(\text{N}^i\text{Pr}_2)_2\}\{\text{N}(\text{Tol})\text{H}_2\text{BTeX}\}$ (**11**) and $\text{Cp}^*\text{Ti}\{\text{MeC}(\text{N}^i\text{Pr}_2)_2\}\{\text{N}(\text{Tol})\text{HBCAr}^{\text{F}}_2\}$ (**12**)^a

Parameter	11	12
Ti(1)–Cp _{cent}	2.06	2.07
Ti(1)–N(1)	1.8813(7)	1.8725(9)
Ti(1)–N(2)	2.0817(7)	2.0950(9)
Ti(1)–N(3)	2.1194(7)	2.0910(8)
Ti(1)–H(1)	1.914(13)	2.009(13)
N(1)–B(1)	1.5466(11)	1.5426(14)
B(1)–H(1)	1.233(13)	1.187(14)
B(1)–H(2)	1.131(13)	n.a.
B(1)–C(8)	1.6473(13)	1.6296(14)
Cp _{cent} –Ti(1)–N(1)	119.0	125.4
Cp _{cent} –Ti(1)–N(2)	114.5	114.0
Cp _{cent} –Ti(1)–N(3)	117.2	116.3
Cp _{cent} –Ti(1)–H(1)	111.6	111.8
N(1)–Ti(1)–N(2)	103.69(3)	99.94(4)
Ti(1)–N(1)–B(1)	91.38(5)	91.62(6)
N(1)–B(1)–C(8)	117.54(7)	113.69(8)

^aNot applicable: n.a.

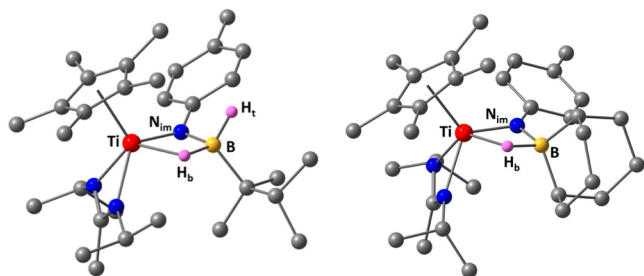


Figure 4. DFT structures of $\text{Cp}^*\text{Ti}\{\text{MeC}(\text{N}^i\text{Pr}_2)_2\}\{\text{N}(\text{Tol})\text{H}_2\text{BTeX}\}$ (**11**, left) and $\text{Cp}^*\text{Ti}\{\text{MeC}(\text{N}^i\text{Pr}_2)_2\}\{\text{N}(\text{Tol})\text{HBC}_8\text{H}_{14}\}$ (**13**, right). C-bound H atoms omitted. Selected distances (Å) for $\text{Cp}^*\text{Ti}\{\text{MeC}(\text{N}^i\text{Pr}_2)_2\}\{\text{N}(\text{Tol})\text{HBCAr}^{\text{F}}_2\}$ (**12**, not shown above): Ti–H_b 1.950, B–H_b 1.297, Ti–N_{im} 1.879, B–N_{im} 1.523; for **11**: Ti–H_b 1.904, B–H_b 1.309, B–H_i 1.231, Ti–N_{im} 1.869, B–N_{im} 1.542; for **13**: Ti–H_b 1.853, B–H_b 1.336, Ti–N_{im} 1.853, B–N_{im} 1.541.

ppm for **11**, **12**, and **13**, respectively (experimental values: 1.4, –7.7, and 10.4 ppm). In solution, **13** was found to partially dissociate to the starting imide and borane. A series of equilibrium constants were measured by NMR spectroscopy in

C_7D_8 (toluene- d_8) between 293 and 333 K. The van't Hoff plot is shown in Figure 5, giving values of $\Delta_r G_{298} = -2.5(1)$ and $\Delta_r H = -9.5(2)$ kcal mol^{–1}.

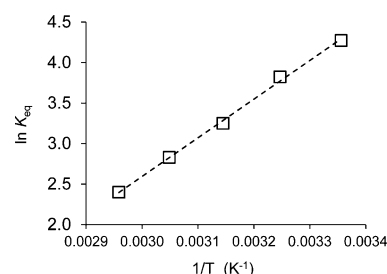


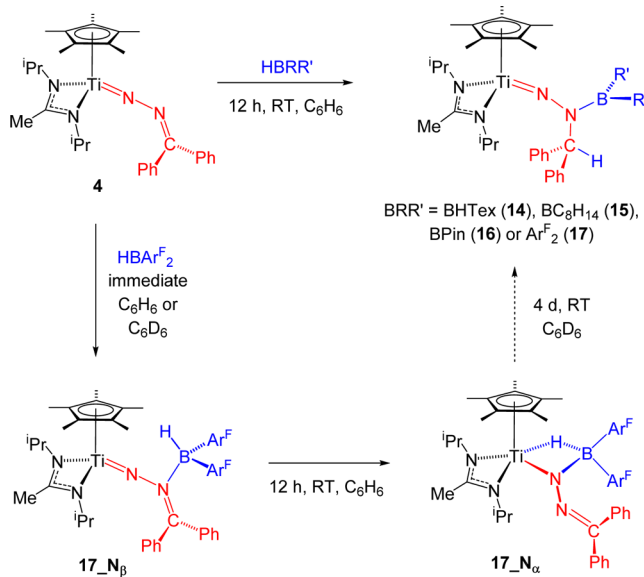
Figure 5. van't Hoff plot for the reaction $\text{Cp}^*\text{Ti}\{\text{MeC}(\text{N}^i\text{Pr}_2)_2\}\{\text{N}(\text{Tol})\}$ (**10**) + 0.5 9-BBN = $\text{Cp}^*\text{Ti}\{\text{MeC}(\text{N}^i\text{Pr}_2)_2\}\{\text{N}(\text{Tol})\text{HBC}_8\text{H}_{14}\}$ (**13**). $\Delta_r H = -9.5(2)$ kcal mol^{–1}, $\Delta_r S = -23.3(7)$ cal mol^{–1} K^{–1}, $\Delta_r G_{298} = -2.5(1)$ kcal mol^{–1} ($R^2 = 0.998$).

Table S1 in the SI lists the computed $\Delta_r G_{298}$ values (kcal mol^{–1}) for the formation of **11** (–23.5), **12** (–19.1), and **13** (0.8) from **10** and the respective dimeric boranes. These are consistent with only $\text{Cp}^*\text{Ti}\{\text{MeC}(\text{N}^i\text{Pr}_2)_2\}\{\text{N}(\text{Tol})\text{HBC}_8\text{H}_{14}\}$ (**13**) being involved in an equilibrium. The $\Delta_r G_{298}$ values starting from the monomeric boranes followed the same trend but were shifted to more negative values by ca. –7 to –10 kcal mol^{–1}. Overall, 1,2-addition of B–H to Ti–N_{im} with the primary borane H₂BTeX is slightly more thermodynamically favored than with the electron-deficient secondary borane, HBCAr^F₂; the bulkier and less Lewis acidic dialkyl borane HBC₈H₁₄ is by far the least favorable.

Reactions of $\text{Cp}^*\text{Ti}\{\text{MeC}(\text{N}^i\text{Pr}_2)_2\}(\text{NNCPh}_2)$ (4**) with boranes.** As mentioned in the Introduction (cf. Figure 1), reactions of alkylidene hydrazides with silanes have given either alkylidene hydrazide(1–)-hydride products (**1**, starting from $\text{Cp}^*_2\text{Ti}(\eta^2\text{-NNCHTol})$) or products of net 1,3 Si–H bond addition across the N–N=CPh₂ moiety (**5**, starting from **4**). This latter reaction is proposed to involve a transient hydride intermediate analogous to **1**. Interestingly, the reactions of **4** with boranes (Scheme 2) formed three types of reaction product, or apparent intermediate, depending on the specific borane, but none of these is directly analogous to either **1** or **5**.

Reaction of **4** with H₂BTeX, 9-BBN, or HBPIn leads to a homologous series of products, $\text{Cp}^*\text{Ti}\{\text{MeC}(\text{N}^i\text{Pr}_2)_2\}\{\text{NN}(\text{BR}_2)\text{CHPh}_2\}$ (BR₂ = BHTex (**14**), BC₈H₁₄ (**15**), or BPIn

Scheme 2. Reactions of $\text{Cp}^*\text{Ti}\{\text{MeC}(\text{N}^i\text{Pr})_2\}(\text{NNCPh}_2)$ (**4**) with Boranes (shown in their monomeric forms)



(**16**) which were isolated on the preparative scale in 50–70% yield after workup. When followed by low temperature NMR spectroscopy in C_7D_8 , no intermediates were observed. Compounds **14**–**16** are borylhydrazido(2–) compounds which are formed by the net 1,2 addition of B–H across the $\text{N}_\beta=\text{CPh}_2$ bond of **4**. Compound **14** is an oil, but the others formed diffraction-quality crystals. The solid state structures and selected metric data for **15** and **16** are given in Figure 6 and Table 2 and discussed below. The solution NMR data are consistent with the solid state structures. In particular, a singlet of intensity 1 H for CHPh_2 is found between 5.55 and 5.75 ppm in the ^1H NMR spectra (the corresponding CHPh_2 signal in $\text{Cp}^*\text{Ti}\{\text{MeC}(\text{N}^i\text{Pr})_2\}[\text{N}(\text{PhSiH}_2)\text{N}(\text{CHPh}_2)]$ (**5**, Ar = Ph, R = H) was found at 5.23 ppm). The ^{11}B spectra each show a single resonance between 44 and 53 ppm, consistent with three-coordinate boron atoms. The IR spectra showed no significant absorptions between 1600 and 2500 cm^{-1} , indicating the absence of B–H bonds in the products.

Compounds **15** and **16** (Figure 6) possess three-legged piano stool geometries at titanium. These are the first examples of borylhydrazido(2–) complexes. The average $\text{Ti}(1)\text{--N}(1)$

Table 2. Selected Bond Distances (Å) and Angles (deg) for $\text{Cp}^*\text{Ti}\{\text{MeC}(\text{N}^i\text{Pr})_2\}[\text{NN}(\text{BC}_6\text{H}_{14})\text{CHPh}_2]$ (**15**) and $\text{Cp}^*\text{Ti}\{\text{MeC}(\text{N}^i\text{Pr})_2\}[\text{NN}(\text{BPin})\text{CHPh}_2]$ (**16**)^a

Parameter	15	16
Ti(1)–Cp _{cent}	2.08	2.08
Ti(1)–N(1)	1.7256(16)	1.7280(8)
Ti(1)–N(3)	2.1052(18)	2.1071(8)
Ti(1)–N(4)	2.119(2)	2.1243(8)
N(1)–N(2)	1.380(2)	1.3723(11)
N(2)–B(1)	1.407(3)	1.4186(13)
B(1)–O(1)	n.a.	1.3794(12)
B(1)–O(2)	n.a.	1.3798(12)
B(1)–C(18)	1.577(3)	n.a.
B(1)–C(14)	1.583(3)	n.a.
Cp _{cent} –Ti(1)–N(1)	124.9	124.8
Cp _{cent} –Ti(1)–N(3)	116.9	119.7
Cp _{cent} –Ti(1)–N(4)	117.2	121.5
Ti(1)–N(1)–N(2)	172.82(14)	168.09(6)
N(1)–N(2)–B(1)	122.67(16)	119.69(8)
N(1)–N(2)–C(1)	113.55(15)	118.30(7)
C(1)–N(2)–B(1)	123.44(16)	119.69(8)

^aNot applicable: n.a.

distance of 1.727(2) Å is shorter compared to that of the starting $\text{Cp}^*\text{Ti}\{\text{MeC}(\text{N}^i\text{Pr})_2\}(\text{NNCPh}_2)$ (**4**) (1.751(2) Å) and comparable to the Ti– N_α distances in the homologous hydrazides $\text{Cp}^*\text{Ti}\{\text{MeC}(\text{N}^i\text{Pr})_2\}(\text{NNMe}_2)$ (**10**, 1.723(2) Å) and $\text{Cp}^*\text{Ti}\{\text{MeC}(\text{N}^i\text{Pr})_2\}(\text{NNPhR}')$ ($\text{R}' = \text{Me}$ or Ph , 1.734(2) Å in both cases).²³ The N(1)–N(2) distances in **15** and **16** are the same within error, and comparable to those in $\text{Cp}^*\text{Ti}\{\text{MeC}(\text{N}^i\text{Pr})_2\}(\text{NNPhR}')$ (**10** has a longer $\text{N}_\alpha\text{--N}_\beta$ bond because N_β is pyramidal). The sums of the N(1)–N(2)–R angles ($360.0(2)$ and $359.7(5)^\circ$) establish a planar geometry at N(2), as is also found for $\text{Cp}^*\text{Ti}\{\text{MeC}(\text{N}^i\text{Pr})_2\}(\text{NNPhR}')$. The N(2)–B(1) bond length in **16** is slightly longer ($\Delta = 0.012(3)$ Å) than in **15** because of competing π -donation from the Pin group O atoms. The other metric parameters for **15** and **16** are within the usual ranges and comparable to previous hydrazides $\text{Cp}^*\text{Ti}\{\text{MeC}(\text{N}^i\text{Pr})_2\}(\text{NNRR}')$.

The reaction of **4** with HBARF_2 differs from those described above. When followed on the NMR tube scale, the immediately first-formed product is an adduct $\text{Cp}^*\text{Ti}\{\text{MeC}(\text{N}^i\text{Pr})_2\}[\text{NN}(\text{HBA}^{\text{F}_2})\text{CPh}_2]$ (**17_Nβ**) with the borane datively coordinated

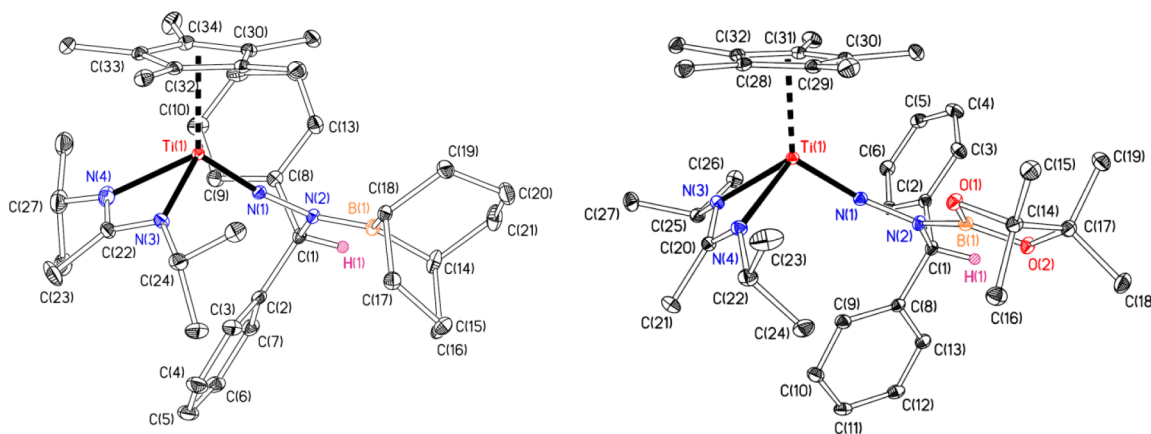


Figure 6. Displacement ellipsoid plots (25% probability) of $\text{Cp}^*\text{Ti}\{\text{MeC}(\text{N}^i\text{Pr})_2\}[\text{NN}(\text{BC}_6\text{H}_{14})\text{CHPh}_2]$ (**15**, left) and $\text{Cp}^*\text{Ti}\{\text{MeC}(\text{N}^i\text{Pr})_2\}[\text{NN}(\text{BPin})\text{CHPh}_2]$ (**16**, right). C-bound H atoms omitted for clarity except H(1) which is drawn as a sphere of an arbitrary radius.

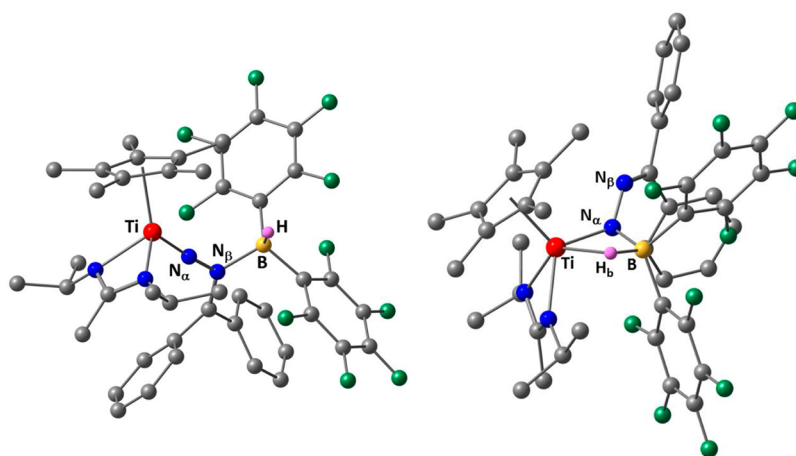


Figure 7. DFT structures of $\text{Cp}^*\text{Ti}\{\text{MeC}(\text{N}^i\text{Pr})_2\}\{\text{NN}(\text{HBAr}^{\text{F}}_2)\text{CPh}_2\}$ ($17_{\text{N}\beta}$, left) and $\text{Cp}^*\text{Ti}\{\text{MeC}(\text{N}^i\text{Pr})_2\}\{\text{N}(\text{HBAr}^{\text{F}}_2)\text{NCPh}_2\}$ ($17_{\text{N}\alpha}$, right). C-bound H atoms omitted. Selected distances (Å) for $17_{\text{N}\beta}$: Ti– N_α 1.732, N_α – N_β 1.318, N_β –B 1.607, B–H 1.219; for $17_{\text{N}\alpha}$: Ti– H_b 1.940, Ti– N_α 1.785, N_α – N_β 1.351, N_α –B 1.553, B– H_b 1.295.

to the N_β atom. This compound was spectroscopically characterized by NMR and solution IR spectroscopy. In particular the ^{11}B NMR spectrum has a single resonance at -8.5 ppm consistent with a four-coordinate boron atom, while the IR spectrum showed a terminal $\nu(\text{B}-\text{H})$ band at 2591 cm^{-1} . Over several hours at room temperature, $17_{\text{N}\beta}$ converts to a more stable isomer, $\text{Cp}^*\text{Ti}\{\text{MeC}(\text{N}^i\text{Pr})_2\}\{\text{N}(\text{HBAr}^{\text{F}}_2)\text{NCPh}_2\}$ ($17_{\text{N}\alpha}$) with the borane bound to N_α . This is an analogue of the structurally characterized tolylimido adduct $\text{Cp}^*\text{Ti}\{\text{MeC}(\text{N}^i\text{Pr})_2\}\{\text{N}(\text{Tol})\text{BAr}^{\text{F}}_2\}$ (**12**).

Compound $17_{\text{N}\alpha}$ is stable for at least 12–18 h in solution and was isolated on the preparative scale as an analytically pure, orange oil in 62% yield. Its ^{11}B NMR shift of -9.7 ppm also indicates a four-coordinate boron atom, while the observed frequency for the $\nu(\text{B}-\text{H})$ band in the IR spectrum at 1945 cm^{-1} clearly indicates a bridging hydride. The corresponding values in **12** were -7.7 ppm and 1939 cm^{-1} for the ^{11}B chemical shift and $\nu(\text{B}-\text{H})$, respectively. The through-space relationships were determined using ROESY ($^1\text{H}-^1\text{H}$) and HOESY ($^1\text{H}-^{19}\text{F}$) techniques. The DFT structures of $17_{\text{N}\beta}$ and $17_{\text{N}\alpha}$ are shown in Figure 7. The computed $\nu(\text{B}-\text{H})$ values of 2468 and 1915 cm^{-1} , respectively, are in agreement with the experimental trends. Finally, over four or more days at room temperature, $17_{\text{N}\alpha}$ rearranges to $\text{Cp}^*\text{Ti}\{\text{MeC}(\text{N}^i\text{Pr})_2\}\{\text{NN}(\text{BAr}^{\text{F}}_2)\text{CHPh}_2\}$ (**17**), analogous to **14**–**16**, as indicated by ^1H and ^{13}C NMR resonances at 6.15 and 77.1 ppm for the NCHPh_2 group and a ^{11}B NMR shift of 33.5 ppm for three-coordinate boron.

Table S2 of the SI lists the computed $\Delta_r G$ values for the formation of $17_{\text{N}\beta}$, $17_{\text{N}\alpha}$ and **17** from **4** and 0.5 equiv of dimeric $[\text{HBAr}^{\text{F}}_2]_2$. The values of -7.0 , -7.1 , and $-15.5\text{ kcal mol}^{-1}$, respectively, indicate that the final 1,2-addition product **17** is the thermodynamic isomer and that both adducts (on N_β and N_α) are thermodynamically viable. The calculations are not able to confidently distinguish between $17_{\text{N}\beta}$ and $17_{\text{N}\alpha}$ in terms of relative stability, whereas the experimental NMR data are unambiguous in finding that $17_{\text{N}\alpha}$ is the more stable of the two. DFT calculations were also carried out on the corresponding N_β and N_α adducts for the reactions with 0.5 equiv of 9-BBN (i.e., $15_{\text{N}\beta}$ and $15_{\text{N}\alpha}$) or 1 equiv of HBPIn (i.e., $16_{\text{N}\beta}$ and $16_{\text{N}\alpha}$), as well as the observed products themselves (**15** and **16**, Table S2 of the SI). In these cases, formation of the final products **15** and **16** is clearly exergonic

($\Delta_r G = -19.9$ and $-15.9\text{ kcal mol}^{-1}$), but the N_β and N_α adducts are endergonic or only very slightly exergonic, consistent with them not being observed. The different stabilities of the adducts for HBAr^{F}_2 are attributed to the higher Lewis acidity of the boron in this case.

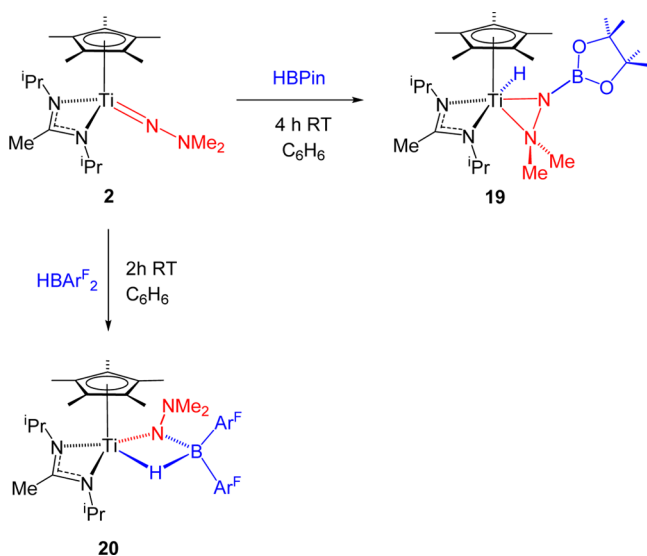
Based on the experimentally observed species and the computed energies of the different adducts, we are able to propose a mechanism for the reactions of **4** with the various boranes. The reactions probably start with coordination of HBR_2 to the sp^2 hybridized β -nitrogen as observed in the case of $17_{\text{N}\beta}$. This would be consistent with the known electronic structure of **4**, the HOMO of which has a large N_β lone pair contribution as well as Ti– N_α bonding character (note that the N_α – N_β – CPh_2 angle in **4** is 120.2°).^{3e} The same type of HOMO is found in $\text{Cp}^*\text{Ti}\{\text{MeC}(\text{N}^i\text{Pr})_2\}(\text{NNMe}_2)$ (**10**, sp^3 hybridized N_β)²³, which is known to react exclusively at N_β with alkyl halides RCH_2X ($\text{R} = \text{H}, \text{Me}$, or Ph , $\text{X} = \text{Br}$ or I), formally a source of $[\text{H}_2\text{CR}]^+$, which is valence isoelectronic with HBR_2 . Other terminal dimethylhydrazides also react with alkyl halides or triflates at N_β and have been structurally characterized for titanium²⁴ and also molybdenum.²⁵ In their studies of molybdenum hydrazides of relevance to the Chatt cycle for N_2 fixations, Tuzek et al. showed that protonation at N_β can be kinetically preferred but that a rapid 1,2-proton shift can occur to form the N_α -protonated counterpart which is thermodynamically more stable.²⁶

From the β -nitrogen adduct it seems that either hydride transfer to CPh_2 or HBR_2 group migration to N_α can occur. In the case of HBAr^{F}_2 the α -nitrogen adduct is sufficiently thermodynamically stable to form. In addition, this borane has the most stabilized B–H bond, as indicated, for example, by the structural, IR, and DFT data for $\text{Cp}^*\text{Ti}\{\text{MeC}(\text{N}^i\text{Pr})_2\}\{\text{N}(\text{Tol})\text{HBAr}^{\text{F}}_2\}$ (**12**) where hydride transfer from B toward Ti is the least advanced. The other boranes form less stable/endergonic N_α adducts and are better hydride donors. Experimentally, $17_{\text{N}\alpha}$ eventually converts to **17**, as indicated by the dotted arrow in Scheme 2. Overall, this requires both a boron atom shift from N_α to N_β and also hydride transfer to CPh_2 . The most plausible pathway for this transformation from the kinetic to the thermodynamic product is via $17_{\text{N}\beta}$, although alternative pathways cannot be excluded on the currently available evidence.

It is interesting to compare the reactions of **4** with PhRSiH_2 , which form products of 1,3-addition to the $\text{N}=\text{N}=\text{CPh}_2$ ligand (**5**, Figure 1), and with HBR_2 giving **14**–**17**. In the case of the poorly Lewis acidic silanes, addition to **4** (and **10**) always proceeds via concerted 1,2-addition to $\text{Ti}-\text{N}_\alpha$, generating titanium hydride species from which hydride transfer to the electrophilic CPh_2 can take place. With HBR_2 1,2-addition to $\text{Ti}-\text{N}_\alpha$ is certainly thermodynamically accessible (cf. the formation of **11**–**13** for example), but these systems appear not to transfer their hydride completely in most cases, preferring to form the ubiquitous $\text{M}-\text{H}-\text{B}$ bridges. In contrast, electrophilic attack at N_β does not stabilize the $\text{B}-\text{H}$ bond in this way, allowing for the facile hydride transfer seen for H_2BTeX , 9-BBN, and HBPin .

Reactions of $\text{Cp}^*\text{Ti}\{\text{MeC}(\text{N}^i\text{Pr})_2\}(\text{NNMe}_2)$ (2**) with HBPin and HBAr^{F_2} .** The reactions of $\text{Cp}^*\text{Ti}\{\text{MeC}(\text{N}^i\text{Pr})_2\}(\text{NNMe}_2)$ (**2**) with 9-BBN, HBPin , and HBAr^{F_2} all lead to different final product types (H_2BTeX gave a mixture of unknown products, none of which could be isolated). No reaction occurred between $\text{Cp}^*\text{Ti}\{\text{MeC}(\text{N}^i\text{Pr})_2\}(\text{NNPh}_2)$ (**18**) and any of the boranes, except for 9-BBN at elevated temperatures. The reaction of **2** with HBPin (Scheme 3)

Scheme 3. Reactions of $\text{Cp}^*\text{Ti}\{\text{MeC}(\text{N}^i\text{Pr})_2\}(\text{NNMe}_2)$ (**2**) with HBPin and HBAr^{F_2}



gave complete $\text{B}-\text{H}$ bond cleavage, forming $\text{Cp}^*\text{Ti}\{\text{MeC}(\text{N}^i\text{Pr})_2\}(\text{H})\{\text{N}(\text{BPin})\text{NMe}_2\}$ (**19**), which, when followed on the NMR tubes scale in C_6D_6 , is the sole product. It was isolated in 53% yield as a green solid on scale-up. Diffraction-quality crystals were grown from benzene, and the solid state structure is shown in Figure 8 along with selected distances and angles.

Compound **19** is a κ^2 -borylhydrazide(1-)-hydride compound, directly analogous to the compounds $\text{Cp}^*\text{Ti}\{\text{MeC}(\text{N}^i\text{Pr})_2\}(\text{H})\{\text{N}(\text{SiH}_2\text{R})\text{NMe}_2\}$ (**3**, Figure 1) formed between **10** and primary silanes. The solid state structures of three examples of **3** have been crystallographically characterized, and the metric data for **19** are very similar. For example, the $\text{Ti}(1)-\text{N}(1)$ and $\text{N}(1)-\text{N}(2)$ distances in **19** are 1.9664(10) and 1.4399(14) Å, respectively, and in the compounds **3** the average values are 1.960 (range 1.952(1)–1.963(3)) and 1.449 (range 1.441(3)–1.460(4)) Å. These distances are all substantially

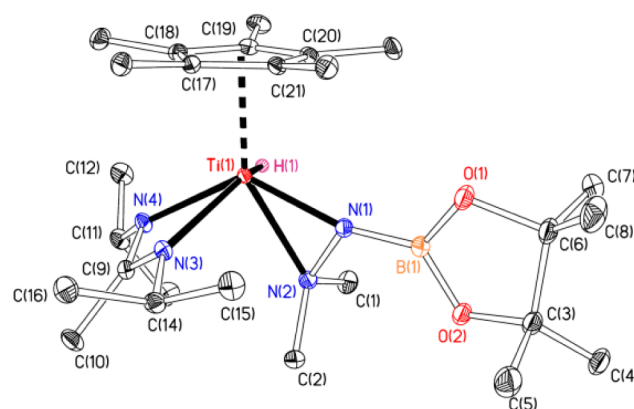


Figure 8. Displacement ellipsoid plot (25% probability) of $\text{Cp}^*\text{Ti}\{\text{MeC}(\text{N}^i\text{Pr})_2\}(\text{H})\{\text{N}(\text{BPin})\text{NMe}_2\}$ (**19**). C-bound H atoms are omitted for clarity; H(1) is drawn as a sphere of arbitrary radius. Selected bond distances (Å) and angles (deg): $\text{Ti}(1)-\text{N}(1)$ 1.9664(10), $\text{Ti}(1)-\text{N}(2)$ 2.2173(11), $\text{Ti}(1)-\text{N}(3)$ 2.1835(10), $\text{Ti}(1)-\text{N}(4)$ 2.1893(10), $\text{Ti}(1)-\text{H}(1)$ 1.70(2), $\text{Ti}(1)-\text{Cp}_{\text{cent}}$ 2.08, $\text{N}(1)-\text{N}(2)$ 1.4399(14), $\text{N}(1)-\text{B}(1)$ 1.4183(17); $\text{Cp}_{\text{cent}}-\text{Ti}(1)-\text{N}(1)$ 114.8, $\text{Cp}_{\text{cent}}-\text{Ti}(1)-\text{N}(3)$ 113.2, $\text{Cp}_{\text{cent}}-\text{Ti}(1)-\text{N}(4)$ 116.6, $\text{Ti}(1)-\text{N}(1)-\text{N}(2)$ 79.58(6), $\text{N}(2)-\text{N}(1)-\text{B}(1)$ 119.40(10).

lengthened from those in **10** itself. The hydride H(1) was located in a Fourier map and positionally and isotropically refined. The $\text{Ti}(1)-\text{H}(1)$ distance of 1.70(2) is comparable within error to those in **3** (av. 1.61, range 1.56(4)–1.64(4) Å), given the uncertainties involved with H atom location using X-ray techniques.²⁷ The new $\text{N}(\text{BPin})\text{NMe}_2$ ligand is κ^2 -coordinated, as is usually the case for titanium hydrazido(1-) complexes,^{24a,28} except for especially crowded systems^{28f} or those with β - NPh_2 substituents.^{28i,29}

The solution NMR data for **19** are consistent with the κ^2 -borylhydrazide(1-)-hydride structure being maintained in solution. In particular, the diastereotopic β - NMe_2 groups give rise to two ^1H singlet resonances at 3.01 and 2.81 ppm of 3 H intensity, the hydride is observed as a singlet (1 H intensity) at 5.57 ppm, similar to the shifts found in **3** (range 5.05–5.15 ppm), and the ^{11}B resonance at 23.7 ppm is consistent with three-coordinate boron. DFT calculations were performed on **19** and on an isomer (19_{κ^1}) with a κ^1 - $\text{N}(\text{BPin})\text{NMe}_2$ ligand. Consistent with the corresponding calculations reported for **3**,^{10a} **19** was found to be $-14.6 \text{ kcal mol}^{-1}$ more stable than 19_{κ^1} , and $\Delta_{\text{r}}G$ for the formation of **19** from **2** and HBPin was $-16.7 \text{ kcal mol}^{-1}$.

Compound **19** is also an analogue of the type of hydrazide(1-)-hydride intermediate proposed by DFT (but not experimentally observed) to be formed en route to the borylamide compound **7** (Figure 1). However, **19** was found to be stable for weeks in solution and in the solid state at RT. Upon heating to 70 °C in C_6D_6 decomposition occurs to a mixture of unidentified products. In addition, **19** did not react further with HBPin or other boranes (cf. the reaction with 9-BBN described below).

In contrast to forming **19** with HBPin , the reaction of **2** with HBAr^{F_2} gave $\text{Cp}^*\text{Ti}\{\text{MeC}(\text{N}^i\text{Pr})_2\}(\text{H})\{\text{N}(\text{NMe}_2)\text{HBAr}^{\text{F}_2}\}$ (**20**, Scheme 3) as an analytically pure red oil which we could not crystallize. The NMR and IR data, supported by DFT calculations (Figure 9) indicate the hydride-bridged structure illustrated. This is analogous to those isolated from the reactions of this borane with **10** (forming **12**) and **4** (forming **17**– N_α). The IR spectrum of **20** shows a $\nu(\text{B}-\text{H})$ band at 1990

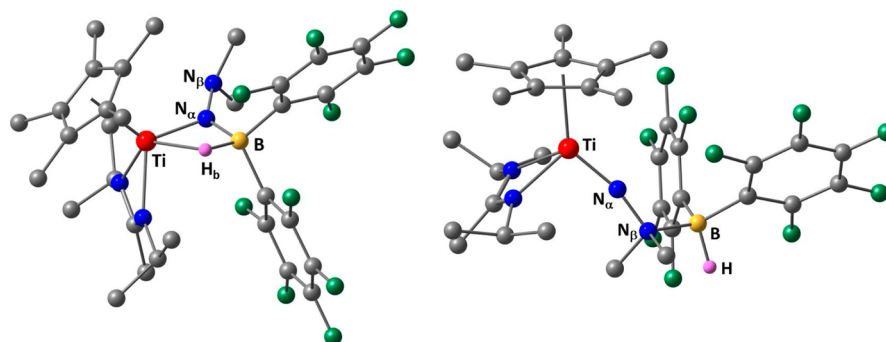
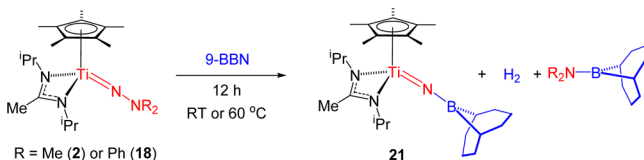


Figure 9. DFT gas phase optimized structures of $\text{Cp}^*\text{Ti}\{\text{MeC}(\text{N}^i\text{Pr})_2\}\{\text{N}(\text{NMe}_2)\text{HBAr}^{\text{F}_2}\}$ (**20**, left) and $\text{Cp}^*\text{Ti}\{\text{MeC}(\text{N}^i\text{Pr})_2\}\{\text{NN}(\text{HBAr}^{\text{F}_2})\text{Me}_2\}$ (**20_N β** , right). C-bound.

cm^{-1} (cf. 1939 cm^{-1} in the crystallographically characterized analogue **12**) for the bridging hydride. The ^{11}B NMR spectrum shows a signal for four-coordinate boron at -6.8 ppm (cf. -7.7 ppm in **12**), and the ^1H NMR shows a singlet at 2.75 ppm of intensity 6 H for the $\beta\text{-NMe}_2$ groups, consistent with them undergoing free rotation/inversion on the NMR time scale because N_β is not coordinated to titanium.

Figure 9 compares the DFT structures of **20** and an isomeric structure $\text{Cp}^*\text{Ti}\{\text{MeC}(\text{N}^i\text{Pr})_2\}\{\text{NN}(\text{HBAr}^{\text{F}_2})\text{Me}_2\}$ (**20_N β**) with HBAr_2 datively coordinated to the nitrogen of the $\beta\text{-NMe}_2$ group, as observed in its reaction with **4** to give **20_N β** as the first-formed product. The computed $\Delta_r G$ for formation of **20_N β** ($-18.6\text{ kcal mol}^{-1}$) shows that its formation is favorable, cf. the reactions of **2** with alkyl halides at N_β to give $[\text{Cp}^*\text{Ti}\{\text{MeC}(\text{N}^i\text{Pr})_2\}(\text{NNMe}_2\text{R})]^+$ as discussed above. However, $\Delta_r G$ for the formation of **20** is $-29.9\text{ kcal mol}^{-1}$, $11.3\text{ kcal mol}^{-1}$ more exergonic. The computed $\nu(\text{B-H})$ frequencies for **20** and **20_N β** are 1912 and 2412 cm^{-1} , again consistent with **20** being the experimentally observed product. We also evaluated by DFT the reaction of **2** with HBAr^{F_2} to form the B-H bond cleavage product $\text{Cp}^*\text{Ti}\{\text{MeC}(\text{N}^i\text{Pr})_2\}(\text{H})\{\text{N}(\text{BAr}^{\text{F}_2})\text{NMe}_2\}$ (analogous to **19**). This is also exergonic with respect to the reactants ($\Delta_r G = -21.8\text{ kcal mol}^{-1}$) but significantly endergonic ($\Delta_r G = +8.1\text{ kcal mol}^{-1}$) with respect to μ -hydride isomer **20**, consistent with the higher Lewis acidity and poorer hydride-donating ability of HBAr^{F_2} in these systems.

Reactions of $\text{Cp}^*\text{Ti}\{\text{MeC}(\text{N}^i\text{Pr})_2\}(\text{NNR}_2)$ ($\text{R} = \text{Me}$ (2**) or Ph (**18**)) with 9-BBN.** The reaction of $\text{Cp}^*\text{Ti}\{\text{MeC}(\text{N}^i\text{Pr})_2\}(\text{NNR}_2)$ ($\text{R} = \text{Me}$ (**2**) or Ph (**18**)) with 9-BBN is summarized in eq 1. Reaction of **2** at room temperature or of **18** at $60\text{ }^\circ\text{C}$



Equation 1

(no reaction at room temperature) with 1 equiv of 9-BBN dimer ($\text{Ti}:\text{B} = 1:2$) in C_6D_6 gave full conversion of the hydrazide and all of the 9-BBN to a 1:1 mixture of $\text{Cp}^*\text{Ti}\{\text{MeC}(\text{N}^i\text{Pr})_2\}(\text{NBC}_8\text{H}_{14})$ (**21**) and the corresponding aminoborane $\text{R}_2\text{NBC}_8\text{H}_{14}$ ($\text{R} = \text{Me}$ or Ph).³⁰ An additional singlet at 4.46 ppm was assigned to eliminated H_2 . The reaction for **2** was successfully scaled up. The aminoborane $\text{Me}_2\text{NBC}_8\text{H}_{14}$ was separated by careful high vacuum sub-

limation ($85\text{--}90\text{ }^\circ\text{C}$, $2 \times 10^{-5}\text{ mbar}$), leaving **21** as an analytically pure, green powder. Diffraction-quality crystals of **21** were grown from hexane. The solid state structure is shown in Figure 10 together with selected bond distances and angles.

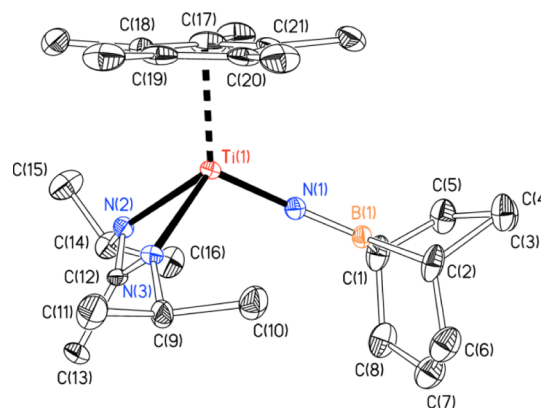


Figure 10. Displacement ellipsoid plot (20% probability) of $\text{Cp}^*\text{Ti}\{\text{MeC}(\text{N}^i\text{Pr})_2\}(\text{NBC}_8\text{H}_{14})$ (**21**). H atoms are omitted for clarity. Selected bond distances (Å) and angles (deg): $\text{Ti}(1)\text{--N}(1)$ $1.731(3)$, $\text{Ti}(1)\text{--N}(2)$ $2.091(4)$, $\text{Ti}(1)\text{--N}(3)$ $2.065(4)$, $\text{Ti}(1)\text{--Cp}_{\text{cent}}$ 2.07 , $\text{N}(1)\text{--B}(1)$ $1.402(4)$, $\text{B}(1)\text{--C}(1)$ $1.523(12)$, $\text{B}(1)\text{--C}(2)$ $1.580(8)$; $\text{Cp}_{\text{cent}}\text{--Ti}(1)\text{--N}(1)$ 118.9 , $\text{Cp}_{\text{cent}}\text{--Ti}(1)\text{--N}(2)$ 122.4 , $\text{Cp}_{\text{cent}}\text{--Ti}(1)\text{--N}(3)$ 122.3 , $\text{Ti}(1)\text{--N}(1)\text{--B}(1)$ $178.4(3)$, $\text{N}(2)\text{--Ti}(1)\text{--N}(1)$ $107.65(19)$, $\text{N}(3)\text{--Ti}(1)\text{--N}(1)$ $108.6(2)$.

On scale up in benzene at $60\text{ }^\circ\text{C}$, compound **18** reacted quantitatively with 1 equiv of 9-BBN dimer to form **21**, along with $\text{Ph}_2\text{NBC}_8\text{H}_{14}$ and H_2 . It was not possible to separate $\text{Ph}_2\text{NBC}_8\text{H}_{14}$ from **21**: the lower volatility of this aminoborane led to longer sublimation times and higher temperatures, giving thermal degradation of **21**. Use of only 0.5 equiv of 9-BBN ($\text{Ti}:\text{B}$ ratio of 1:1) in the NMR tube scale reactions gave incomplete conversion, confirming the stoichiometry required by eq 1.

Compound **21** is a rare example of a borylimide, for which only a few examples have previously been reported.^{5a,c,31} The ^{11}B NMR spectrum shows a singlet at 52.8 ppm (calculated 52.9 ppm for the DFT model of **21**) consistent with three-coordinate boron and very similar to the value of 54.5 ppm for the borylamide ligand in $\text{Ti}(\text{N}_2\text{N}^{\text{Me}})\{\text{N}(\text{H})\text{BC}_8\text{H}_{14}\}(\text{NPh}_2)$ (**7**, Figure 1).^{5b} The IR spectrum shows no bands attributable to either $\nu(\text{B-H})$ or $\nu(\text{Ti-H})$. The solid state structure of **21** (Figure 11) possesses a three-legged piano stool geometry. The parameters associated with the $\text{Cp}^*\text{Ti}\{\text{MeC}(\text{N}^i\text{Pr})_2\}$ moiety are within the expected ranges. The $\text{Ti}(1)\text{--N}(1)$ bond length

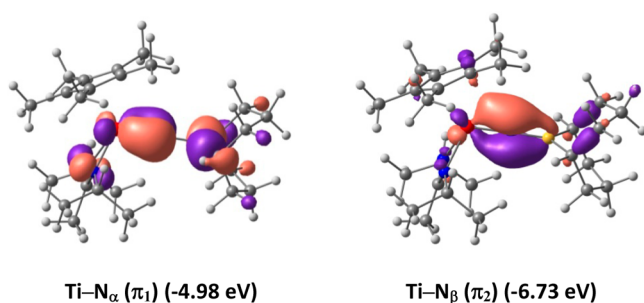


Figure 11. Two Ti–N α π -bonding MOs of Cp^{*}Ti{MeC(NⁱPr)₂}(NBC₈H₁₄) (**21**) and their energies. Isosurfaces are drawn at the 0.032 au level.

of 1.731(3) Å and linear Ti(1)–N(1)–B(1) angle 178.4(3)° is indicative of a Ti–N α triple bond as confirmed by DFT calculations (cf. Figure 11). The Ti(1)–N(1) distance lies in the range of typical values for titanium arylimido compounds (ca. 1.70–1.74)²¹ and can be compared with previously reported xylimido, hydrazido, and *tert*-butoxyimido titanium homologues, Cp^{*}Ti{MeC(NⁱPr)₂}(NR) (R = Xyl (1.738(2) Å), NPh₂ (1.734(2) Å), NMePh (1.734(2) Å), NMe₂ (1.723(2) Å), and O^tBu (1.709(3) Å)), as well as that in Cp^{*}Ti{MeC(NⁱPr)₂}{NN(BC₈H₁₄)CHPh₂} (**15**) above.

Mindiola has reported two examples of titanium borylimides, namely **22** (from the corresponding parent imide with 2 equiv of NaHBEt₃)^{5a} and **23** (by reaction of a metalated nitride with ClBCat).^{5c} The Ti–N α distances of 1.722(3) and 1.7312(2) Å, respectively, are equivalent within error to that in **21**.

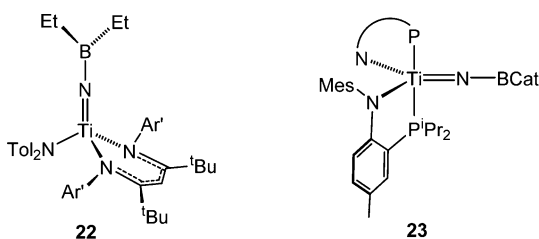
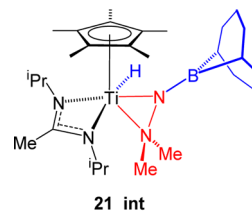


Figure 11 shows the two principal Ti–N α π -bonding molecular orbitals (denoted π_1 and π_2 ; σ -bonding MO not shown) calculated for **21**. This is consistent with the Ti–N α triple bond description. The energy difference of 1.75 eV between π_1 and π_2 is substantial because of stabilization of the latter Ti–N α π -interaction by delocalization to the otherwise vacant 2p atomic orbital of the boron atom, as also indicated by the relatively short N(1)–B(1) distance of 1.402(4) Å.

Further NMR tube scale experiments were carried out to probe the reaction of Cp^{*}Ti{MeC(NⁱPr)₂}(NNR₂) with 9-BBN. Thus, following the reaction for **2** at room temperature established that the evolutions of **21** and Me₂NBC₈H₁₄ were correlated (along with evolution of H₂). Analogous results were found for **18**, and no free HNMe₂ or HNPh₂ or their borane adducts were observed. When HNPh₂ and 0.5 equiv of 9-BBN were heated together under the same concentration as in the NMR experiments with **18**, the formation of Ph₂NBC₈H₁₄ was found to be much slower (48 h cf. 12 h starting from **18** and 9-BBN). No intermediates were observed in the reactions of **18** either at 60 °C or at lower temperatures. In the case of **2**, however, monitoring the reaction with 9-BBN at 0 °C in C₇D₈ showed the formation of a new species **21_int**, which featured resonances comparable to those of Cp^{*}Ti{MeC(NⁱPr)₂}(H){N(BPin)NMe₂} (**19**), suggesting the formation of a

borylhydrazide(1-)-hydride compound. Warming up the NMR sample containing **21_int** led to the consumption of it and unreacted 9-BBN and formation of **21**, Me₂NBC₈H₁₄, and H₂, as in the room temperature reactions. Attempts to isolate **21_int** were unsuccessful, and upon evaporation of the volatiles from the reaction mixtures unknown products were obtained.



The ¹¹B NMR spectrum of **21_int** showed a downfield resonance at 28.1 ppm. The ¹H NMR spectrum showed a singlet of intensity 1 H at 6.30 ppm which did not correlate to any H or C atoms and is assigned as Ti–H. The β -NMe₂ groups gave rise to overlapping broad signals (relative intensity 3 H each) at 2.75 and 2.65 ppm. The structure of **21_int** was

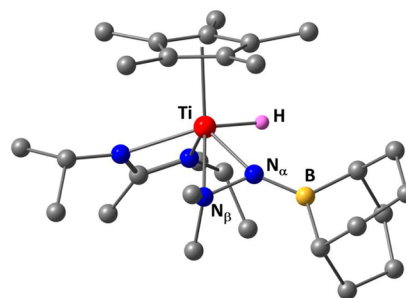


Figure 12. DFT structure of Cp^{*}Ti{MeC(NⁱPr)₂}(H){N(BC₈H₁₄)-NMe₂} (**21_int**). C-bound H atoms omitted. Selected distances (Å): Ti–H 1.660, Ti–N α 1.956, N α –N β 1.416, B–N α 1.400.

computed by DFT and is shown in Figure 12. The calculated ¹¹B NMR shift for **21_int** of 32.0 ppm is in good agreement with the experimental value. Unfortunately, we have been unable to establish by experiment or DFT further details of a possible mechanism leading from **21_int** and 9-BBN to the product borylimide and amidoborane. It is known in dehydrocoupling of amine-boranes in general that B–N coupling and H₂ elimination can be correlated in various ways.³² Further speculation at this stage is inappropriate.

CONCLUSIONS

In this contribution we have significantly expanded upon our initial report of the reaction of the titanium hydrazide Ti(N₂N^{Me})(NNPh₂)(py) with 9-BBN to give Ti(N₂N^{Me}){N(H)BC₈H₁₄}(NPh₂) (**7**, Figure 1) and its homologue with HBMe₂. The wider range of imido and hydrazido compounds available with the Cp^{*}{MeC(NⁱPr)₂} ligand set, which is tolerant to a variety of borane substituents, allowed us to make a broader assessment of the types of adducts, 1,2-addition, and B–H/N α –N β cleavage processes accessible in this chemistry. In the case of Cp^{*}Ti{MeC(NⁱPr)₂}(NTol) only hydride-bridged adducts Cp^{*}Ti{MeC(NⁱPr)₂}{N(Tol)HBRR'} without B–H bond cleavage were formed. These are structurally related to Lancaster's Cp₂Hf{N(H)HBAr^F₂} (**9**) but are in contrast to Walter's (η -C₅H₂^tBu₃)₂Th(H){N(BC₈H₁₄)Tol}, which exists as a terminal hydride-borylamide derivative, and also Chen's **8**

(Figure 1), although in this case the hydride was stabilized by further reaction with 9-BBN.

The reactions of $\text{Cp}^*\text{Ti}\{\text{MeC}(\text{N}^i\text{Pr})_2\}\{\text{NNCPh}_2\}$ (**4**) with boranes follow fundamentally different pathways to the one with silanes which gives Si–H 1,3-addition products to the NNCPh_2 ligand, forming **3** (Figure 1). The observed β -nitrogen and α -nitrogen adducts formed with HBAr^{F}_2 prior to the final product $\text{Cp}^*\text{Ti}\{\text{MeC}(\text{N}^i\text{Pr})_2\}\{\text{NN}(\text{BAr}^{\text{F}}_2)\text{CHPh}_2\}$ (**17**) allow insight into the possible mechanism of the reactions of the other boranes studied with **4**. The Lewis acidity of boron, the availability of a β -nitrogen lone pair in **4**, and the general absence of hydride formation by 1,2-addition to Ti– N_α explain the reaction pathways taken. The reaction of $\text{Cp}^*\text{Ti}\{\text{MeC}(\text{N}^i\text{Pr})_2\}\{\text{NNMe}_2\}$ (**2**) with HBPIn is the most similar, of all the reactions of boranes reported, to the corresponding one with primary silanes. The B–H bond cleavage product is stabilized by β - NMe_2 coordination, as in the silane reaction products. With HBAr^{F}_2 the effect of the higher Lewis acidity of boron is evidenced by the incomplete transfer of hydride to titanium. The reaction of **2** with 9-BBN is especially interesting in terms of forming a rare example of a borylimido compound, and it suggests that this type of reaction may be accessible for other early transition metal hydrazido complexes.

EXPERIMENTAL SECTION

General methods and instrumentation. All manipulations were carried out using standard Schlenk line or glovebox techniques under an atmosphere of argon or dinitrogen. Solvents were either degassed by sparging with dinitrogen and dried by passing through a column of the appropriate drying agent³³ or refluxed over sodium (toluene), potassium (THF), Na/K alloy (Et_2O) or and distilled. Deuterated solvents were dried over sodium (C_7D_8) or potassium (C_6D_6) distilled under reduced pressure and stored under argon in Teflon valve ampules. NMR samples were prepared under dinitrogen in 5 mm Wilmad 507-PP tubes fitted with J. Young Teflon valves. ^1H , $^{13}\text{C}\{^1\text{H}\}$, $^{11}\text{B}\{^1\text{H}\}$ and $^{19}\text{F}\{^1\text{H}\}$ spectra were recorded on a Bruker Ascend 400 NMR spectrometer, a Bruker Avance III 500 NMR spectrometer or on a Bruker AVE 500 spectrometer fitted with a ^{13}C cryoprobe. Unless otherwise stated, all NMR spectra were recorded at 298 K. ^1H and $^{13}\text{C}\{^1\text{H}\}$ and spectra were referenced internally to residual protio-solvent (^1H) or solvent (^{13}C) resonances, and are reported relative to tetramethylsilane ($\delta = 0$ ppm). ^{19}F and ^{11}B NMR spectra were referenced externally to CFCl_3 and $\text{Et}_2\text{O}\cdot\text{BF}_3$ respectively. Assignments were confirmed as necessary with the use of two-dimensional ^1H – ^1H , ^{13}C – ^1H , ^1H – ^{19}F and ^{19}F – ^{19}F correlation experiments. Chemical shifts are quoted in δ (ppm) and coupling constants in Hz. Unless otherwise stated, IR spectra were recorded on a Thermo Scientific Nicolet iS5 FTIR spectrometer and samples prepared in a drybox using NaCl plates as a Nujol mull or as a thin film. The data are quoted in wavenumbers (cm^{-1}). Mass spectra were recorded by the mass spectrometry service of Oxford University's Department of Chemistry. Elemental analyses were carried out by the Elemental Analysis Service at the London Metropolitan University.

Starting materials. $\text{Cp}^*\text{Ti}\{\text{MeC}(\text{N}^i\text{Pr})_2\}\{\text{NR}\}$ ($\text{R} = ^i\text{Bu}$ or Tol (**10**)),^{22d} $\text{Cp}^*\text{Ti}\{\text{MeC}(\text{N}^i\text{Pr})_2\}\{\text{NO}^i\text{Bu}\}$,^{4a,b} $\text{Cp}^*\text{Ti}\{\text{MeC}(\text{N}^i\text{Pr})_2\}\{\text{NNR}_2\}$ ($\text{R}_2 = \text{Me}_2$ (**2**), Ph_2 (**18**) or CPh_2 (**4**)),^{3e,23} HBCy_2 ,¹⁶ H_2BTex ,¹⁵ HBAr^{F}_2 ,^{12,34} HBMe_2 ,¹⁷ $\text{HB}(\text{NAr}^i\text{CH}_2)$,¹⁸ $\text{HB}(\text{N}^i\text{PrCH}_2)_2$ ¹⁹ were synthesized according to literature procedures. Other boranes were obtained from commercial source and used without additional purification.

Syntheses. $\text{Cp}^*\text{Ti}\{\text{MeC}(\text{N}^i\text{Pr})_2\}\{\text{N}(\text{Tol})\text{H}_2\text{BTex}\}$ (**11**). To a stirred solution of $\text{Cp}^*\text{Ti}\{\text{MeC}(\text{N}^i\text{Pr})_2\}\{\text{NTol}\}$ (**10**, 0.300 g, 0.669 mmol) in benzene (10 mL) was added H_2BTex (0.065 g, 0.669 mmol) at RT. The solution was left to stir at RT for 12 h, filtered and volatiles removed under reduced pressure to afford the adduct as a yellow oil. This was triturated with pentane to give **11** as a yellow/brown solid which was washed with cold pentane (3×10 mL) and dried *in vacuo*.

Yield 0.263 g (75%). Diffraction-quality crystals were grown from pentane at RT.

^1H NMR (C_6D_6 , 400.1 MHz, 298 K): δ 7.02 (4 H, overlapping m - $\text{C}_6\text{H}_4\text{Me}$ and o - $\text{C}_6\text{H}_4\text{Me}$), 3.73 (1 H, broad, CH_4Me_2), 3.51 (1 H, broad, CH_4Me_2), 2.23 (3 H, s, $\text{C}_6\text{H}_4\text{Me}$), 2.03 (1 H, m, $\text{BCMe}_2\text{CHMe}_2$), 1.85 (15 H, s, C_5Me_5), 1.66 (3 H, s, MeCN_2), 1.34 (3 H, d, $^3J = 6.5$ Hz, NCH_3MeMe), 1.30 (6 H, d, $\text{BCMe}_2\text{CHMe}_2$), 1.26 (3 H, d, $^3J = 6.5$ Hz, NCH_3MeMe), 1.21 (3 H, d, $^3J = 6.5$ Hz, NCH_3MeMe), 1.15 (3 H, d, $^3J = 6.5$ Hz, NCH_3MeMe), 1.01–0.96 (6 H, overlapping, $\text{BCMe}_2\text{CHMe}_2$). $^{13}\text{C}\{^1\text{H}\}$ NMR (C_6D_6 , 100.6 MHz, 298 K): δ 164.7 (MeCN_2), 154.6 (i - $\text{C}_6\text{H}_4\text{Me}$), 132.4 (p - $\text{C}_6\text{H}_4\text{Me}$), 130.4 (m - $\text{C}_6\text{H}_4\text{Me}$), 122.8 (o - $\text{C}_6\text{H}_4\text{Me}$), 121.8 (C_5Me_5), 50.7 (NCH_3Me_2), 48.7 (NCH_3Me_2), 37.1 ($\text{BCMe}_2\text{CHMe}_2$), 26.0 ($\text{BCMe}_2\text{CHMe}_2$), 25.3 ($\text{BCMe}_2\text{CHMe}_2$), 23.9 (NCH_3MeMe), 23.0 (NCH_3MeMe), 24.31 (NCH_3MeMe), 19.5 (NCH_3MeMe), 18.7 ($\text{BCMe}_2\text{CHMe}_2$), 21.02 ($\text{C}_6\text{H}_4\text{Me}$), 14.9 (MeCN_2), 11.7 (C_5Me_5) ppm. $^{11}\text{B}\{^1\text{H}\}$ NMR (C_6D_6 , 128.4 MHz, 298 K): 1.5 (s) ppm. IR (NaCl plates, Nujol mull, cm^{-1}): 2327 (s, terminal $\nu(\text{B}=\text{H})$), 1908 (m, bridging $\nu(\text{B}=\text{H})$), 1599 (w), 1455 (s), 1378 (s), 1303 (s), 1130 (s), 1110 (s), 1079 (m), 1044 (w), 924 (w), 847 (w), 835 (w), 818 (w), 607 (w). EI-MS: $m/z = 527$ [M – H]⁺ (20%), 324 [M – $\text{N}(\text{Tol})\text{BH}_2\text{Tex}$]⁺ (80%). Anal. found (calcd. for $\text{C}_{31}\text{H}_{54}\text{BN}_3\text{Ti}$): C 67.72 (70.59), H 10.50 (10.32), N 7.32 (7.97). The sample gave persistently low %C, N analysis, even of diffraction-quality crystals.

$\text{Cp}^*\text{Ti}\{\text{MeC}(\text{N}^i\text{Pr})_2\}\{\text{N}(\text{Tol})\text{BHAr}^{\text{F}}_2\}$ (**12**). To a stirred solution of $\text{Cp}^*\text{Ti}\{\text{MeC}(\text{N}^i\text{Pr})_2\}\{\text{NTol}\}$ (**10**, 0.300 g, 0.669 mmol) in benzene (10 mL) was added HBAr^{F}_2 (0.231 g, 0.669 mmol) at RT. The solution was stirred at RT for 12 h, filtered and the volatiles removed under reduced pressure to afford brown oil. This was triturated with pentane to give **12** as a brown solid which was washed with cold pentane (3×10 mL) and dried *in vacuo*. Yield: 0.306 g (60%). Diffraction-quality crystals were grown from pentane at RT.

^1H NMR (C_6D_6 , 400.1 MHz, 298 K): δ 6.94 (2 H, d, $^3J = 8.5$ Hz, m - $\text{C}_6\text{H}_4\text{Me}$), 6.67 (2 H, d, $^3J = 8.5$ Hz, o - $\text{C}_6\text{H}_4\text{Me}$), δ 3.04 (2 H, br. s, CHMe_2), 2.11 (3 H, s, $\text{C}_6\text{H}_4\text{Me}$), 1.78 (15 H, s, C_5Me_5), 1.37 (3 H, s, MeCN_2), 1.09 (6 H, d, $^3J = 6.7$ Hz, CHMe_2), 0.80 (6 H, d, $^3J = 6.7$ Hz, CHMe_2) ppm. $^{13}\text{C}\{^1\text{H}\}$ NMR (C_6D_6 , 100.6 MHz, 298 K): δ 163.6 (MeCN_2), 156.01 (i - $\text{C}_6\text{H}_4\text{Me}$), 148.5 (br. d, $^1J = 236.4$ Hz, o - C_6F_5), 140.3–138.2 (overlapping br. d, p - C_6F_5 and m - C_6F_5), 132.5 (br, i - C_6F_4), 133.3 (p - $\text{C}_6\text{H}_4\text{Me}$), 128.2 (m - $\text{C}_6\text{H}_4\text{Me}$), 122.2 (o - $\text{C}_6\text{H}_4\text{Me}$), 126.6 (C_5Me_5), 49.4 (NCHMe_2), 26.8 (NCHMe_2), 24.3 (NCHMe_2), 19.6 ($\text{C}_6\text{H}_4\text{Me}$), 14.6 (MeCN_2), 12.4 (C_5Me_5) ppm. $^{11}\text{B}\{^1\text{H}\}$ NMR (C_6D_6 , 128.4 MHz, 298 K): -7.7 (s) ppm. $^{19}\text{F}\{^1\text{H}\}$ NMR (470.1 MHz, 298 K): -133.4 (o - C_6F_5), -158.2 (m - C_6F_5), -164.4 (p - C_6F_5). IR (NaCl plates, Nujol mull, cm^{-1}): 1939 (s, $\nu(\text{B}=\text{H})$), 1530 (s), 1410 (m), 1094 (s), 1083 (s), 1015 (s), 971 (w), 833 (s), 813 (w), 662 (w). EI-MS: $m/z = 775$ [M]⁺ (50%). Anal. found (calcd. for $\text{C}_{37}\text{H}_{40}\text{BF}_{10}\text{N}_3\text{Ti}$): C, 57.32 (57.93); H, 5.20 (5.53); N, 5.42 (5.37) %.

$\text{Cp}^*\text{Ti}\{\text{MeC}(\text{N}^i\text{Pr})_2\}\{\text{N}(\text{Tol})\text{HBC}_8\text{H}_{14}\}$ (**13**). To a stirred solution of $\text{Cp}^*\text{Ti}\{\text{MeC}(\text{N}^i\text{Pr})_2\}\{\text{NTol}\}$ (**10**, 0.300 g, 0.669 mmol) in benzene (10 mL) was added 9-BBN (0.085 g, 0.348 mmol) at RT. The solution was left to stir at RT for 12 h, filtered and volatiles removed under reduced pressure to afford **13** as a viscous yellow/brown oil, which could not be crystallized and was washed with cold pentane (3×10 mL) and dried *in vacuo*. Yield: 0.184 g (50%).

^1H NMR (C_6D_6 , 400.1 MHz, 298 K): δ 6.98 (2 H, d, $^3J = 8.5$ Hz, m - $\text{C}_6\text{H}_4\text{Me}$), 6.87 (2 H, d, $^3J = 8.5$ Hz, o - $\text{C}_6\text{H}_4\text{Me}$), δ 3.55 (2 H, br. s, CHMe_2), 2.10 (3 H, s, $\text{C}_6\text{H}_4\text{Me}$), 1.95 (15 H, s, C_5Me_5), 1.66 (3 H, s, MeCN_2), 2.30–1.0 (14 H, overlapping 3*m*, BCH , BCCH and BCCCH), 1.14 (6 H, d, $^3J = 6.7$ Hz, CHMe_2), 1.01 (6 H, d, $^3J = 6.7$ Hz, CHMe_2) ppm. $^{13}\text{C}\{^1\text{H}\}$ NMR (C_6D_6 , 100.6 MHz, 298 K): δ 163.5 (MeCN_2), 158.6 (i - $\text{C}_6\text{H}_4\text{Me}$), 130.8 (p - $\text{C}_6\text{H}_4\text{Me}$), 128.3 (overlapping o - $\text{C}_6\text{H}_4\text{Me}$ and m - $\text{C}_6\text{H}_4\text{Me}$), 125.4 (C_5Me_5), 120.2 (4- $\text{C}_6\text{H}_4\text{Me}$), 49.4 (NCHMe_2), 33.7 (BCCCH), 25.9 (NCHMe_2), 25.1 (NCHMe_2), 24.4 (BCCCH), 20.6 ($\text{C}_6\text{H}_4\text{Me}$), 11.2 (BCH), 13.6 (MeCN_2), 12.5 (C_5Me_5) ppm. $^{11}\text{B}\{^1\text{H}\}$ NMR (C_6D_6 , 128.4 MHz, 298 K): 10.4 (s) ppm. IR (NaCl plates, Nujol mull, cm^{-1}): 1651 (s, $\nu(\text{B}=\text{H})$), 1517 (w), 1376 (w), 1260 (s), 1092 (s), 1093 (s), 1019 (s), 800

(s). EI-MS: $m/z = 551 [M]^+$ (2%). A satisfactory elemental analysis of this oil, which readily dissociates 9-BBN (see the main text), could not be obtained.

$Cp^*Ti\{MeC(N^iPr)_2\}NN(BHTex)CHPh_2$ (14). To a stirred solution of $Cp^*Ti\{MeC(N^iPr)_2\}(NNCPh_2)$ (4, 0.300 g, 0.579 mmol) in benzene (10 mL) was added H_2BTeX (0.057 g, 0.579 mmol) at RT. The solution was stirred for 12 h at RT, filtered and volatiles were removed under reduced pressure. The resultant orange oil was washed with cold pentane and dried *in vacuo* to afford 14 as a viscous yellow oil which could not be crystallized. Yield: 0.260 g (70%).

1H NMR (C_6D_6 , 400.0 MHz, 298 K): δ 7.47 (4 H, d, $^3J = 8.0$ Hz, o - C_6H_5), 7.14 (4 H, m, m - C_6H_5), 7.09 (2 H, m, p - C_6H_5), 5.74 (1 H, s, $CHPh_2$), 3.52 (2 H, app. sept., $^3J = 7.0$ Hz, $NCHMeMe$), 2.05 (15 H, s, C_5Me_5), 1.75 (3 H, s, $MeCN_2$), 1.03 (6 H, d, $^3J = 7.0$ Hz, $NCHMe_2$), 0.88 (7 H, overlapping $BHCHMe_2$ and $BHCHMe_2CHMe_2$), 0.79 (6 H, $BHCHMe_2CHMe_2$), 0.78 (6 H, d, $^3J = 7.0$ Hz, $NCHMe_2$). $^{13}C\{^1H\}$ NMR (C_6D_6 , 100.0 MHz, 298 K): δ 161.2 ($MeCN_2$), 142.4 (i - C_6H_5), 129.4 (o - C_6H_5), 127.4 (p - C_6H_5), 126.4 (m - C_6H_5), 119.3 (C_5Me_5), 66.6 ($CHPh_2$), 49.1 ($NCHMe_2$), 25.2 ($NCHMe_2$), 26.0 ($BHCHMe_2CHMe_2$), 23.7 ($BHCHMe_2CHMe_2$), 23.4 ($BHCHMe_2CHMe_2$), 18.7 ($BHCHMe_2CHMe_2$), 18.6 ($NCHMe_2$), 11.7 (C_5Me_5). $^{11}B\{^1H\}$ NMR (C_6D_6 , 128.4 MHz, 298 K): 46.4 (s) ppm. Anal. found (calcd. for $C_{37}H_{47}BN_4Ti$): C, 72.84 (73.28); H, 9.32 (9.38); N, 9.09 (9.24) %.

$Cp^*Ti\{MeC(N^iPr)_2\}NN(BCH_8H_{14})CHPh_2$ (15). To a stirred solution of $Cp^*Ti\{MeC(N^iPr)_2\}(NNCPh_2)$ (4, 0.338 g, 0.652 mmol) in benzene (10 mL) was added 9-BBN (0.080 g, 0.326 mmol) at RT. The solution was stirred for 12 h at RT, filtered and volatiles were removed under reduced pressure to afford 15 as a brown powder. The product was washed with cold pentane (3×10 mL) and dried *in vacuo*. Yield: 0.280 g (67%). Diffraction-quality crystals were grown from a concentrated benzene solution at RT.

1H NMR (C_6D_6 , 400.0 MHz, 298 K): δ 7.42 (4 H, dd, $^3J = 8.1$ MHz, o - C_6H_5), 7.14 (4 H, m, m - C_6H_5), 7.06 (2 H, m, p - C_6H_5), 5.96 (1 H, s, $CHPh_2$), 3.52 (2 H, app. sept., $^3J = 6.3$ Hz, $NCHMeMe$), 2.30–1.0 (14 H, overlapping 3m, BCH , $BCCCH$ and $BCCCH$), 1.95 (15 H, s, C_5Me_5), 1.73 (3 H, s, $MeCN_2$), 0.96 (6 H, d, $^3J = 6.3$ Hz, $NCHMe_2$), 0.83 (6 H, d, $^3J = 6.3$ Hz, $NCHMe_2$). $^{13}C\{^1H\}$ NMR (C_6D_6 , 100.0 MHz, 298 K): δ 161.4 ($MeCN_2$), 142.4 (i - C_6H_5), 129.4 (o - C_6H_5), 127.4 (p - C_6H_5), 126.4 (m - C_6H_5), 119.7 (C_5Me_5), 68.5 ($CHPh_2$), 48.8 ($NCHMe_2$), 33.4 (BCH), 25.9 ($NCHMe_2$), 25.3 ($NCHMe_2$), 23.4, 22.7 ($BCCCH$, $BCCCH$), 12.2 (C_5Me_5). $^{11}B\{^1H\}$ NMR (C_6D_6 , 128.4 MHz, 298 K): 52.5 (s) ppm. IR (NaCl plates, Nujol mull, cm^{-1}): 1489 (w), 1418 (m), 1325 (w), 1308 (w), 1260 (s), 1214 (w), 1092 (s), 1020 (s) 800 (s), 695 (w), 668 (m). Anal. found (calcd. for $C_{39}H_{57}BN_4Ti$): C, 73.12 (72.88); H, 8.97 (9.15); N, 8.75 (8.62) %.

$Cp^*Ti\{MeC(N^iPr)_2\}NN(Bpin)CHPh_2$ (16). To a stirred solution of $Cp^*Ti\{MeC(N^iPr)_2\}(NNCPh_2)$ (4, 0.210 g, 0.549 mmol) in benzene (10 mL) was added $HBpin$ (0.079 mL, 0.549 mmol) at RT. An immediate color change from dark brown to dark green was observed after 30 min. The solution was filtered and volatiles removed under reduced pressure to give 16 as a brown solid which was washed with cold pentane (3×10 mL) and dried *in vacuo*. Yield: 0.177 g (50%). Diffraction-quality crystals were grown from a concentrated benzene solution at RT.

1H NMR (C_6D_6 , 400.0 MHz, 298 K): δ 7.49 (4 H, dd, $^3J = 7.4$ Hz, o - C_6H_5), 7.19 (4 H, m, m - C_6H_5), 7.11 (2 H, t, p - C_6H_5), 5.55 (1 H, s, $CHPh_2$), 3.62 (2 H, app. sept., $^3J = 6.1$ Hz, $NCHMeMe$), 2.13 (15 H, s, C_5Me_5), 1.81 (3 H, s, $MeCN_2$), 1.14 (6 H, d, $^3J = 6.5$ Hz, $BOCMe_2$), 1.07 (6 H, d, $^3J = 6.1$ Hz, $NCHMe_2$), 0.80 (6 H, d, $^3J = 6.1$ Hz, $NCHMe_2$). $^{13}C\{^1H\}$ NMR (C_6D_6 , 100.0 MHz, 298 K): δ 161.4 ($MeCN_2$), 143.7 (i - C_6H_5), 130.0 (o - C_6H_5), 127.9 (p - C_6H_5), 127.7 (m - C_6H_5), 119.4 (C_5Me_5), 82.9 ($BOCMe_2$), 66.1 ($CHPh_2$), 49.5 ($NCHMe_2$), 26.7 ($NCHMeMe$), 25.5 ($NCHMeMe$), 24.9 ($BOCMe_2$), 12.5 (C_5Me_5), 12.0 ($MeCN_2$). $^{11}B\{^1H\}$ NMR (C_6D_6 , 128.4 MHz, 298 K): δ 44.9 ppm. IR (NaCl plates, Nujol mull, cm^{-1}): 1599 (m), 1462 (s), 1352 (m), 1309 (w), 1260 (m), 1145 (w), 1133 (m), 1083 (m), 1065 (m), 1018 (m), 971 (w), 799 (s), 740 (w) 700

(w), 649 (w). Anal. found (calcd. for $C_{37}H_{55}BN_4O_2Ti$): C, 68.70 (68.57); H, 8.57 (8.59); N, 8.67 (8.49) %.

NMR tube scale synthesis of $Cp^*Ti\{MeC(N^iPr)_2\}NN(HBAR^F_2)CPh_2$ (17_N β). In a glovebox, to a solution of $Cp^*Ti\{MeC(N^iPr)_2\}(NNCPh_2)$ (4, 20 mg, 0.036 mmol) in C_7D_8 (0.3 mL) in an NMR tube equipped with a J. Young Teflon valve was added $HBAR^F_2$ (12.1 mg, 0.036 mmol) in C_7D_8 (0.3 mL). The solution was immediately cooled to ca. 0 °C and transferred to the precooled (internal temperature ca. 0 °C) probe of an NMR instrument. The NMR spectra showed quantitative conversion to 17_N β which was characterized *in situ*.

1H NMR (C_7D_8 , 400.0 MHz, 273 K): δ 7.54 (4 H, dd, $^3J = 6.6$ Hz o - C_6H_5), 6.94 (4 H, m, m - C_6H_5), 6.71 (2 H, m, p - C_6H_5), 3.05 (2 H, app. sept., $^3J = 6.3$ Hz, $NCHMeMe$), 1.89 (15 H, s, C_5Me_5), 1.70 (3 H, s, $MeCN_2$), 0.86 (6 H, d, $^3J = 6.3$ Hz, $NCHMeMe$), 0.75 (6 H, d, $^3J = 6.3$ Hz, $NCHMeMe$). $^{13}C\{^1H\}$ NMR (C_7D_8 , 100.0 MHz, 273 K): δ 164.5 ($MeCN_2$), 137.1 (i - C_6H_5), 128.7 (o - C_6H_5), 126.6 (p - C_6H_5), 124.6 (m - C_6H_5), 123.1 (C_5Me_5), 49.4 ($NCHMeMe$), 25.9–25.4 (overlapping $NCHMeMe$ and $NCHMeMe$), 12.1 (C_5Me_5). $^{11}B\{^1H\}$ NMR (C_7D_8 , 128.4 MHz, 293 K) NMR –8.5 (s) ppm. IR (NaCl cell, toluene, $\nu(B-H)$, cm^{-1}): 2591 (s).

$Cp^*Ti\{MeC(N^iPr)_2\}N(HBAR^F_2)NCPH_2$ (17_N α). To a stirred solution of $Cp^*Ti\{MeC(N^iPr)_2\}(NNCPh_2)$ (4, 0.338 g, 0.652 mmol) in benzene (10 mL) was added $HBAR^F_2$ (0.080 g, 0.652 mmol) at RT. The solution changed color immediately from dark brown to red. After stirring for 12 h at RT, compound $Cp^*Ti\{MeC(N^iPr)_2\}N(HBAR^F_2)NCPH_2$ (17_N α) was isolated, volatiles were removed under reduced pressure and the product was washed with cold pentane and dried *in vacuo*, to yield an orange oil. Yield: 0.346 g (62%).

1H NMR (C_6D_6 , 400.0 MHz, 298 K): δ 7.09 (4 H, dd, $^3J = 6.5$ Hz, o - C_6H_5), 6.99 (4 H, m, m - C_6H_5), 6.89 (2 H, m, p - C_6H_5), 3.14 (2 H, app. sept., $^3J = 6.5$ Hz, $NCHMeMe$), 1.71 (15 H, s, C_5Me_5), 1.57 (3 H, s, $MeCN_2$), 1.04 (6 H, d, $^3J = 6.5$ Hz, $NCHMeMe$), 0.99 (6 H, d, $^3J = 6.5$ Hz, $NCHMeMe$). $^{13}C\{^1H\}$ NMR (C_6D_6 , 100.0 MHz, 298 K): δ 168.8 ($MeCN_2$), 145.7 (3,5- C_6F_5), 141.8 (4- C_6F_5), 137.6 (2,6- C_6F_5), 129.8 (i - C_6H_5), 129.5 (o - C_6H_5), 126.6 (p - C_6H_5), 124.6 (m - C_6H_5), 121.4 (C_5Me_5), 49.2 ($NCHMeMe$), 23.9 ($NCHMeMe$), 24.3 ($NCHMeMe$), 16.4 ($MeCN$), 11.2 (C_5Me_5). $^{11}B\{^1H\}$ NMR (C_6D_6 , 128.4 MHz, 298 K): δ –9.7 ppm. $^{19}F\{^1H\}$ NMR –130.7 (2 F, 2,6- C_6F_5), –162.0 (1 F, 4- C_6F_5), –166.1 (2 F, 3,5- C_6F_5). IR (NaCl cell, toluene, cm^{-1}): 1945 (s, $\nu(B-H)$), 1795, 1803 (w), 1640 (s) 1509 (s), 1321 (m), 1086 (m), 892 (m), 766 (m), 697 (s), 621 (m). Anal. found (calcd. for $C_{43}H_{43}BF_{10}N_4Ti$): C, 59.74 (59.62); H, 5.01 (5.01); N, 6.48 (6.54) %. The NMR assignments were confirmed using HOESY (1H – ^{19}F) spectroscopy.

NMR tube scale synthesis of $Cp^*Ti\{MeC(N^iPr)_2\}NN(BAR^F_2)CHPh_2$ (17). Over 4 days at RT, solutions of $Cp^*Ti\{MeC(N^iPr)_2\}N(HBAR^F_2)NCPH_2$ (17_N α) in toluene or benzene convert to $Cp^*Ti\{MeC(N^iPr)_2\}NN(BAR^F_2)CHPh_2$ (17) along with a number of unidentified side-products which could not be separated on the preparative scale. Compound 17 was therefore characterized by NMR spectroscopy in comparison with the crystallographically characterized analogues $Cp^*Ti\{MeC(N^iPr)_2\}NN(Bpin)CHPh_2$ (16) and $Cp^*Ti\{MeC(N^iPr)_2\}NN(BCH_8H_{14})CHPh_2$ (15), *vide infra*. In a glovebox, to a solution of $Cp^*Ti\{MeC(N^iPr)_2\}(NNCPh_2)$ (4, 20 mg, 0.036 mmol) in C_7D_8 (0.3 mL) in an NMR tube equipped with a J. Young Teflon valve was added $HBAR^F_2$ (12.1 mg, 0.036 mmol) in C_7D_8 (0.3 mL). After 4 days at RT the NMR spectra showed the formation of 17 which was characterized by NMR spectroscopy.

1H NMR (C_6D_6 , 400.0 MHz, 298 K): δ 7.31 (4 H, dd, $^3J = 6.7$ Hz, o - C_6H_5), 7.03 (4 H, m, m - C_6H_5), 6.83 (2 H, m, p - C_6H_5), 6.15 (1 H, s, $CHPh_2$), 3.24 (2 H, broad, $NCHMeMe$), 1.85 (15 H, s, C_5Me_5), 1.71 (3 H, s, $MeCN_2$), 0.79 (6 H, d, $NCHMeMe$), 0.66 (6 H, d, $NCHMeMe$). $^{13}C\{^1H\}$ NMR (C_6D_6 , 100.0 MHz, 298 K): δ 161.4 ($MeCN_2$), 142.4 (i - C_6H_5), 129.4–127.4 (overlapping o - C_6H_5 , p - C_6H_5 and m - C_6H_5), 121.4 (C_5Me_5), 77.1 ($CHPh_2$), 48.5 ($NCHMeMe$), 25.5 ($NCHMeMe$), 24.5 ($NCHMeMe$), 12.5 ($MeCN$), 11.8 (C_5Me_5). $^{11}B\{^1H\}$ NMR (C_6D_6 , 128.4 MHz, 298 K) 33.5 ppm.

$\text{Cp}^*\text{Ti}\{\text{MeC}(\text{N}^i\text{Pr})_2\}(\text{H})\{\text{N}(\text{Bpin})\text{NMe}_2\}$ (**19**). To a stirred solution of $\text{Cp}^*\text{Ti}\{\text{MeC}(\text{N}^i\text{Pr})_2\}(\text{NNMe}_2)$ (**2**, 0.300 g, 0.785 mmol) in benzene (10 mL) was added HBpin (0.112 mL, 0.785 mmol) at RT. An immediate color change from dark brown to dark green was observed. After 4 h the solution was then filtered, the volatiles removed under reduced pressure and the resultant green powder (**19**) washed with cold pentane (3 \times 10 mL) and dried *in vacuo*. Yield: 0.210 g (53%). Diffraction-quality crystals were grown from a concentrated benzene solution at room RT.

^1H NMR (C_6D_6 , 400.1 MHz, 298 K): δ 5.57 (1 H, s, Ti–H), 3.54 (1 H, app. sept., app. 3J = 6.4 Hz, CH_2MeMe), 3.16 (1 H, app. sept., app. 3J = 6.4 Hz, CH_2MeMe), 3.01 (3 H, s, NNMeMe), 2.81 (3 H, s, NNMeMe), 2.27 (15 H, s, C_5Me_5), 1.67 (3 H, s, MeCN_2), 1.24 (3 H, d, 3J = 6.5 Hz, NCH_2MeMe), 1.15 (3 H, d, 3J = 6.5 Hz, NCH_2MeMe), 1.11 (6 H, s, BOCMe_2), 1.10 (3 H, d, 3J = 6.5 Hz, NCH_2MeMe), 1.09 (6 H, s, BOCMe_2 of Bpin), 1.04 (3 H, d, 3J = 6.5 Hz, NCH_2MeMe) ppm. $^{13}\text{C}\{^1\text{H}\}$ NMR (C_6D_6 , 100.6 MHz, 298 K): δ 172.5 (MeCN_2), 120.1 (C_5Me_5), 81.5 (BOCMe_2), 59.9 (NNMeMe), 49.8 (NNMeMe), 48.8 (NCH_2MeMe), 47.8 (NCH_2MeMe), 27.4 (NCH_2MeMe), 26.8 (NCH_2MeMe), 25.7 (NCH_2MeMe), 24.9 (BOCMe_2), 24.7 (NCH_2MeMe), 13.9 (C_5Me_5), 12.7 (MeCN_2) ppm. $^{11}\text{B}\{^1\text{H}\}$ NMR (C_6D_6 , 128.4 MHz, 298 K): δ 23.7 (s) ppm. IR (NaCl plates, Nujol mull, cm^{-1}): 1504 (s, ν (Ti–H)), 1336 (w), 1261 (m), 1201 (s) 1147 (s), 1107 (m), 1020 (m), 967 (m), 858 (m), 793 (s), 664 (m). EI-MS: m/z = 510 [M^+] (2%). Anal. found (calcd. for $\text{C}_{26}\text{H}_{51}\text{BN}_4\text{O}_2\text{Ti}$): C, 61.18 (61.00); H, 10.07 (10.18); N, 10.98 (10.73)%

$\text{Cp}^*\text{Ti}\{\text{MeC}(\text{N}^i\text{Pr})_2\}(\text{H})\{\text{N}(\text{NMe}_2)\text{HBAr}^F_2\}$ (**20**). To a stirred solution of $\text{Cp}^*\text{Ti}\{\text{MeC}(\text{N}^i\text{Pr})_2\}(\text{NNMe}_2)$ (**2**, 0.300 g, 0.750 mmol) in benzene (10 mL) was added HBAr^F_2 (0.260 g, 0.750 mmol) at RT. An immediate color change from dark brown to dark red was observed. After 2 h the solution was then filtered; volatiles were removed under reduced pressure to afford a red oil which could not be crystallized. This was washed with cold pentane (3 \times 10 mL) and dried *in vacuo*. Yield: 0.367 g (80%).

^1H NMR (C_6D_6 , 400.0 MHz, 298 K): δ 3.31 (2 H, app. sept., 3J = 6.5 Hz, NCHMe_2), 2.75 (6 H, s, NNMe_2), 1.85 (15 H, s, C_5Me_5), 1.63 (3 H, s, MeCN_2), 0.89 (6 H, d, 3J = 6.5 Hz, NCHMe_2), 0.81 (6 H, d, 3J = 6.5 Hz, NCHMe_2) ppm. $^{13}\text{C}\{^1\text{H}\}$ NMR (C_6D_6 , 100 MHz, 293 K): δ 161.9 (MeCN_2), 149.1 (br d, 1J = 236.4 Hz, $o\text{-C}_6\text{F}_5$), 140.5 (overlapping br. d, $p\text{-C}_6\text{F}_5$ and $m\text{-C}_6\text{F}_5$), 132.5 (br, $i\text{-C}_6\text{F}_5$), 120.2 (C_5Me_5), 55.4 (NNMe_2), 49.1 (NCHMe_2), 26.3 (NCHMe_2), 24.3 (NCHMe_2), 13.9 (C_5Me_5), 12.7 (MeCN_2) ppm. $^{11}\text{B}\{^1\text{H}\}$ NMR (C_6D_6 , 128.4 MHz, 293 K): δ –6.8 ppm. $^{19}\text{F}\{^1\text{H}\}$ NMR (470.1 MHz, 298 K): δ –128.4 ($o\text{-C}_6\text{F}_5$), –158.7 ($m\text{-C}_6\text{F}_5$), –164.2 ($p\text{-C}_6\text{F}_5$). IR (NaCl plates, Nujol mull, cm^{-1}): 2185 (w), 1990 (s, ν (B–H)), 1857 (m), 1802 (m), 1648 (s) 1264 (w), 1120 (m). Anal. found (calcd. for $\text{C}_{32}\text{H}_{40}\text{BF}_{10}\text{N}_4\text{Ti}$): C, 52.39 (52.70); H, 5.30 (5.53); N, 7.49 (7.68) %.

$\text{Cp}^*\text{Ti}\{\text{MeC}(\text{N}^i\text{Pr})_2\}(\text{NBC}_8\text{H}_{14})$ (**21**). To a stirred solution of $\text{Cp}^*\text{Ti}\{\text{MeC}(\text{N}^i\text{Pr})_2\}(\text{NNMe}_2)$ (**2**, 0.338 g, 0.884 mmol) in benzene (10 mL) was added 9-BBN (0.216 g, 0.884 mmol) all at RT. The solution was left to stir at RT for 12 h, filtered and volatiles removed under reduced pressure to afford **21** and $\text{Me}_2\text{NBC}_8\text{H}_{14}$ (characterized by comparison with the literature NMR data^{30a}) quantitatively in a 1:1 ratio as a sticky brown oil that was washed with pentane (2 \times 10 mL) to remove some of the $\text{Me}_2\text{NBC}_8\text{H}_{14}$. The remaining aminoborane was separated by sublimation (85–90 $^\circ\text{C}$, 2×10^{-5} mbar, 2 h) onto a dry ice/acetone coldfinger leaving **21** as a green powder. Yield: 0.150 g (37%). Diffraction-quality crystals were grown from a concentrated hexane solution at –30 $^\circ\text{C}$.

^1H NMR (C_6D_6 , 400.1 MHz, 298 K): δ 3.53 (2 H, app. sept., app. 3J = 6.5 Hz, CHMe_2), 2.15 (15 H, s, C_5Me_5), 1.65 (3 H, s, MeCN_2), 2.30–1.0 (14 H, overlapping 3m, BCH, BCCH and BCCCH), 1.00 (6 H, d, 3J = 6.5 Hz, CHMe_2), 0.91 (6 H, d, 3J = 6.5 Hz, CHMe_2) ppm. $^{13}\text{C}\{^1\text{H}\}$ NMR (C_6D_6 , 100.6 MHz, 298 K): δ 167.2 (MeCN_2), 121.96 (C_5Me_5), 49.4 (CHMe_2), 34.7 (BCCH), 26.1 (CHMe_2), 24.7 (CHMe_2), 24.4 (BCCCH), 12.3 (BCH), 13.0 (C_5Me_5), 11.6 (MeCN_2) ppm. ^{11}B NMR (C_6D_6 , 128.4 MHz, 298 K): δ 52.8 (s) ppm. IR (NaCl plates, Nujol mull, cm^{-1}): 1601 (w), 1337 (w), 1313 (w), 1280 (s), 1212 (w), 1093 (s), 1018 (s), 800 (s). EI-MS: m/z =

459 [M^+] (2%). Anal. found (calcd. for $\text{C}_{26}\text{H}_{46}\text{BN}_3\text{Ti}$): C, 67.98 (67.95); H, 10.09 (9.84); N, 9.15 (8.82)%.

$\text{Cp}^*\text{Ti}\{\text{MeC}(\text{N}^i\text{Pr})_2\}(\text{NBC}_8\text{H}_{14})$ (**21**) from $\text{Cp}^*\text{Ti}\{\text{MeC}(\text{N}^i\text{Pr})_2\}(\text{NNPh}_2)$ (**18**). To a stirred solution of $\text{Cp}^*\text{Ti}\{\text{MeC}(\text{N}^i\text{Pr})_2\}(\text{NNPh}_2)$ (**18**, 0.448 g, 0.884 mmol) in benzene (10 mL) was added 9-BBN dimer (0.216 g, 0.884 mmol) all at RT. The solution was left to stir at RT for 12 h at 60 $^\circ\text{C}$, filtered and volatiles removed under reduced pressure to afford **21** and $\text{Ph}_2\text{NBC}_8\text{H}_{14}$ (characterized by comparison with the literature NMR data^{30b}) quantitatively in a 1:1 ratio as a sticky brown oil, which could not be separated. The mixture was fully characterized on the NMR scale.

NMR tube scale synthesis of $\text{Cp}^*\text{Ti}\{\text{MeC}(\text{N}^i\text{Pr})_2\}(\text{H})\{\text{N}(\text{BC}_8\text{H}_{14})\text{NMe}_2\}$ (21_int**).** To a solution of $\text{Cp}^*\text{Ti}\{\text{MeC}(\text{N}^i\text{Pr})_2\}(\text{NNMe}_2)$ (**2**, 0.020 mg, 0.053 mmol) in C_6D_6 (0.3 mL) in an NMR tube equipped with a J. Young Teflon valve was added 9-BBN (0.128 mg, 0.054 mmol) in C_7D_8 (0.3 mL). The reaction was monitored by ^1H and ^{11}B NMR spectroscopy. After 1 h at 0 $^\circ\text{C}$, the ^1H NMR spectrum showed complete conversion to **21_int** and unreacted 9-BBN.

^1H NMR (C_6D_6 , 400.1 MHz, 298 K): δ 6.30 (1 H, s, Ti–H), 3.51 (1 H, app. sept., app. 3J = 6.5 Hz, CH_2MeMe), 3.34 (2 H, app. sept., app. 3J = 6.5 Hz, CH_2MeMe), 2.75 (3 H, broad s, NNMeMe), 2.65 (3 H, broad s, NNMeMe), 2.23 (15 H, s, C_5Me_5), 1.81 (3 H, s, MeCN_2), 2.30–1.0 (14 H, overlapping 3m, BCH, BCCH and BCCCH), 1.23 (6 H, d, 3J = 6.5 Hz, CHMe_2), 1.17 (6 H, d, 3J = 6.5 Hz, CHMe_2) ppm. $^{13}\text{C}\{^1\text{H}\}$ NMR (C_6D_6 , 100.6 MHz, 298 K): δ 160.9 (MeCN_2), 122.6 (C_5Me_5), 56.7 (NNMeMe), 51.5 (NNMeMe), 48.1 (NCH_2MeMe), 47.6 (NCH_2MeMe), 33.5 (BCCH), 25.9–24.4 (overlapping NCH_2MeMe , NCH_2MeMe , NCH_2MeMe and NCH_2MeMe), 24.4 (BCCCH), 14.3 (BCH), 13.4 (C_5Me_5), 11.1 (MeCN_2) ppm. $^{11}\text{B}\{^1\text{H}\}$ NMR (C_6D_6 , 128.4 MHz, 298 K): δ 28.1 (s) ppm.

X-ray data collection and processing procedures. Crystals were mounted on glass fibers using perfluoropolyether oil and cooled rapidly in a stream of cold N_2 using an Oxford Cryosystems Cryostream unit. Diffraction data were measured using either an Enraf-Nonius KappaCCD or Agilent Technologies Supernova diffractometer using Mo $K\alpha$ or Cu $K\alpha$ radiation, respectively. As appropriate, absorption and decay corrections were applied to the data and equivalent reflections merged.³⁵ The structures were solved with SIR92³⁶ or Superflip,³⁷ and further refinements and all other crystallographic calculations were performed using the CRYSTALS program suite.³⁸ The CIF files contain specific details for the refinements of the individual structures. The CCDC codes for the structures in this paper are CCDC 1407872, 1407873, and 1556743–1556746.

Computational Details. Geometry optimizations were performed with the Gaussian09 package (rev. D.01)³⁹ at the B3PW91 level of hybrid density functional theory in the gas phase with the titanium atom represented by the relativistic effective core potential (RECP) from the Stuttgart group and the associated basis set,⁴⁰ augmented by an f polarization function,⁴¹ and the remaining atoms represented by a def2-svp basis set.⁴² Dispersion was taken into account both at the optimization and single point stages using Grimme's d3(bj) corrections⁴³ as implemented in Gaussian09. In addition, the solvent (benzene) influence was taken into consideration in the single point calculations on the gas-phase optimized geometry with SCRF calculations within the SMD model and a def2-qzvp basis set for all atoms. Gibbs free energies and enthalpies were obtained by summing the SMD energy, the gas-phase Gibbs or enthalpy contribution at 298.15 K obtained from the geometry optimizations, and the d3(bj) correction. The total SCF and other energies are given in Table S3. NMR chemical shifts were computed using the GIAO method⁴⁴ as implemented in Gaussian09 at the B3PW91 level. All atoms were described with the pcSseg-2 NMR basis sets of Jensen.⁴⁵ The ^{11}B NMR shifts are referenced with respect to the experimental value of 0.0 ppm for $\text{BF}_3(\text{Et}_2\text{O})$. The Cartesian coordinates for the DFT structures are provided as Supporting Information.

■ ASSOCIATED CONTENT

■ Supporting Information

The Supporting Information is available free of charge on the ACS Publications website at DOI: 10.1021/acs.organomet.7b00477.

Remaining details of the DFT calculations (PDF)

Computed Cartesian coordinates of all of the DFT structures reported in this study (XYZ)

■ Accession Codes

CCDC 1407872, 1407873, and 1556743–1556746 contain the supplementary crystallographic data for this paper. These data can be obtained free of charge via www.ccdc.cam.ac.uk/data_request/cif, or by emailing data_request@ccdc.cam.ac.uk, or by contacting The Cambridge Crystallographic Data Centre, 12 Union Road, Cambridge CB2 1EZ, UK; fax: +44 1223 336033.

■ AUTHOR INFORMATION

■ Corresponding Authors

*E-mail: eric.clot@umontpellier.fr.

*E-mail: philip.mountford@chem.ox.ac.uk.

■ ORCID

Eric Clot: 0000-0001-8332-5545

Philip Mountford: 0000-0001-9869-9902

■ Notes

The authors declare no competing financial interest.

■ ACKNOWLEDGMENTS

This work was funded by the EPSRC (grant reference EP/K503113/1 (LCS)), the University of Oxford Clarendon Fund (SM), and the University of Oxford SCG Innovation Fund. We thank the University of Oxford's Advanced Research Computing facility for access to supercomputer and other resources. The authors declare no competing financial interests.

■ REFERENCES

- (1) (a) Wigley, D. E. *Prog. Inorg. Chem.* **1994**, 42, 239–482. (b) Duncan, A. P.; Bergman, R. G. *Chem. Rev.* **2002**, 2, 431–445. (c) Mountford, P. *Chem. Commun.* **1997**, 2127–2134. (d) Gade, L. H.; Mountford, P. *Coord. Chem. Rev.* **2001**, 216–217, 65–97. (e) Hazari, N.; Mountford, P. *Acc. Chem. Res.* **2005**, 38, 839–849. (f) Bolton, P. D.; Mountford, P. *Adv. Synth. Catal.* **2005**, 347, 355–366. (g) Fout, A. R.; Kilgore, U. J.; Mindiola, D. J. *Chem. - Eur. J.* **2007**, 13, 9428–9440. (h) Odom, A. L. *Dalton Trans.* **2005**, 225–233. (i) Schafer, L. L.; Lee, A. V. *Eur. J. Inorg. Chem.* **2007**, 2007, 2245–2255. (j) Müller, T. E.; Hultsch, K. C.; Yus, M.; Foubelo, F.; Tada, M. *Chem. Rev.* **2008**, 108, 3795–3892. (k) Lorber, C. *Coord. Chem. Rev.* **2016**, 308, 76–96.
- (2) (a) Mindiola, D. J. *Angew. Chem., Int. Ed.* **2008**, 47, 1557–1559. (b) Dilworth, J. R. *Coord. Chem. Rev.* **2017**, 330, 53–94.
- (3) (a) Kool, L. B.; Rausch, M. D.; Alt, H. G.; Herberhold, M.; Hill, A. F.; Thewalt, U.; Wolf, B. J. *Chem. Soc., Chem. Commun.* **1986**, 408–409. (b) Polse, J. L.; Kaplan, A. W.; Andersen, R. A.; Bergman, R. G. *J. Am. Chem. Soc.* **1998**, 120, 6316–6328. (c) Kaplan, A. W.; Polse, J. L.; Ball, G. E.; Andersen, R. A.; Bergman, R. G. *J. Am. Chem. Soc.* **1998**, 120, 11649–11662. (d) Hanna, T. E.; Keresztes, I.; Lobkovsky, E.; Bernskoetter, W. H.; Chirik, P. J. *Organometallics* **2004**, 23, 3448–3458. (e) Tiong, P. J.; Groom, L. R.; Clot, E.; Mountford, P. *Chem. - Eur. J.* **2013**, 19, 4198–4216.
- (4) (a) Schwarz, A. D.; Nova, A.; Clot, E.; Mountford, P. *Chem. Commun.* **2011**, 47, 4926–4928. (b) Schwarz, A. D.; Nova, A.; Clot, E.; Mountford, P. *Inorg. Chem.* **2011**, 50, 12155–12171. (c) Groom, L. R.; Schwarz, A. D.; Nova, A.; Clot, E.; Mountford, P. *Organometallics* **2013**, 32, 7520–7539.
- (5) (a) Thompson, R.; Chen, C.-H.; Pink, M.; Wu, G.; Mindiola, D. J. *J. Am. Chem. Soc.* **2014**, 136, 8197–8200. (b) Stevenson, L. C.; Mellino, S.; Clot, E.; Mountford, P. *J. Am. Chem. Soc.* **2015**, 137, 10140–10143. (c) Grant, L. N.; Pinter, B.; Kurogi, T.; Carroll, M. E.; Wu, G.; Manor, B. C.; Carroll, P. J.; Mindiola, D. J. *Chem. Sci.* **2017**, 8, 1209–1224.
- (6) (a) Walsh, P. J.; Carney, M. J.; Bergman, R. G. *J. Am. Chem. Soc.* **1991**, 113, 6343–6345. (b) Herrmann, H.; Fillol, J. L.; Wadepohl, H.; Gade, L. H. *Angew. Chem., Int. Ed.* **2007**, 46, 8426–8430. (c) Selby, J. D.; Manley, C. D.; Feliz, M.; Schwarz, A. D.; Clot, E.; Mountford, P. *Chem. Commun.* **2007**, 4937–4939. (d) Schofield, A. D.; Nova, A.; Selby, J. D.; Schwarz, A. D.; Clot, E.; Mountford, P. *Chem. - Eur. J.* **2011**, 17, 265–285. (e) Schofield, A. D.; Nova, A.; Selby, J. D.; Manley, C. D.; Schwarz, A. D.; Clot, E.; Mountford, P. *J. Am. Chem. Soc.* **2010**, 132, 10484–10497. (f) Gehrmann, T.; Scholl, S. A.; Fillol, J. L.; Wadepohl, H.; Gade, L. H. *Chem. - Eur. J.* **2012**, 18, 3925–3942. (g) Unruangsri, J.; Morgan, H.; Schwarz, A. D.; Schofield, A. D.; Mountford, P. *Organometallics* **2013**, 32, 3091–3107.
- (7) (a) Walsh, P. J.; Hollander, F. J.; Bergman, R. G. *J. Am. Chem. Soc.* **1988**, 110, 8729–8731. (b) Cummins, C. C.; Baxter, S. M.; Wolczanski, P. T. *J. Am. Chem. Soc.* **1988**, 110, 8731–8733.
- (8) (a) Bennett, J. L.; Wolczanski, P. T. *J. Am. Chem. Soc.* **1994**, 116, 2179–2180. (b) Schaller, C. P.; Bonanno, J. B.; Wolczanski, P. T. *J. Am. Chem. Soc.* **1994**, 116, 4133–4134. (c) Schaller, C. P.; Cummins, C. C.; Wolczanski, P. T. *J. Am. Chem. Soc.* **1996**, 118, 591–611. (d) Bennett, J. L.; Wolczanski, P. T. *J. Am. Chem. Soc.* **1997**, 119, 10696–10719. (e) Hoyt, H. M.; Michael, F. E.; Bergman, R. G. *J. Am. Chem. Soc.* **2004**, 126, 1018–1019. (f) Hoyt, H. M.; Bergman, R. G. *Angew. Chem., Int. Ed.* **2007**, 46, 5580–5582. (g) Polse, J. L.; Andersen, R. A.; Bergman, R. G. *J. Am. Chem. Soc.* **1998**, 120, 13405–13414. (h) Toomey, H. E.; Pun, D.; Veiro, L. F.; Chirik, P. J. *Organometallics* **2008**, 27, 872–879.
- (9) (a) Crevier, T. J.; Mayer, J. M. *Angew. Chem., Int. Ed.* **1998**, 37, 1891–1893. (b) Parkin, G.; Bercaw, J. E. *J. Am. Chem. Soc.* **1989**, 111, 391–393. (c) Gountchev, T. I.; Tilley, T. D. *J. Am. Chem. Soc.* **1997**, 119, 12831–12841. (d) Sweeney, Z. K.; Polse, J. L.; Bergman, R. G.; Andersen, R. A. *Organometallics* **1999**, 18, 5502–5510. (e) Chu, J.; Lu, E.; Chen, Y.; Leng, X. *Organometallics* **2013**, 32, 1137–1140. (f) Chu, J.; Han, X.; Kefalidis, C. E.; Zhou, J.; Maron, L.; Leng, X.; Chen, Y. *J. Am. Chem. Soc.* **2014**, 136, 10894–10897. (g) Thompson, R.; Tran, B. A.; Ghosh, S.; Chen, C.-H.; Pink, M.; Gao, X.; Carroll, P. J.; Baik, M.-H.; Mindiola, D. J. *Inorg. Chem.* **2015**, 54, 3068–3077.
- (10) (a) Tiong, P. J.; Nova, A.; Schwarz, A. D.; Selby, J. D.; Clot, E.; Mountford, P. *Dalton Trans.* **2012**, 41, 2277–2288. (b) Tiong, P. J.; Nova, A.; Clot, E.; Mountford, P. *Chem. Commun.* **2011**, 47, 3147–3149.
- (11) Stevenson, L. C. D. Phil. Thesis, University of Oxford, 2015.
- (12) Parks, D. J.; Piers, W. E.; Yap, G. P. A. *Organometallics* **1998**, 17, 5492–5503.
- (13) Zhou, E.; Ren, W.; Hou, G.; Zi, G.; Fang, D.-C.; Walter, M. D. *Organometallics* **2015**, 34, 3637–3647.
- (14) Jacobs, E. A.; Fuller, A.; Coles, S. J.; Jones, G. A.; Tizzard, G. J.; Wright, J. A.; Lancaster, S. J. *Chem. - Eur. J.* **2012**, 18, 8647–8658.
- (15) Schwier, J. R.; Brown, H. C. *J. Org. Chem.* **1993**, 58, 1546–1552.
- (16) Zhdanko, A.; Maier, M. E. *Eur. J. Org. Chem.* **2014**, 2014, 3411–3422.
- (17) Pelter, A.; Smith, K.; Brown, H. C. *Borane Reagents*; Academic Press: New York, 1988.
- (18) Hadlington, T. J.; Abdalla, J. A. B.; Tirfoin, R.; Aldridge, S.; Jones, C. *Chem. Commun.* **2016**, 52, 1717–1720.
- (19) Wallis, C. J.; Dyer, H.; Vendier, L.; Alcaraz, G.; Sabo-Etienne, S. *Angew. Chem., Int. Ed.* **2012**, 51, 3646–3648.
- (20) Hermanek, S. *Chem. Rev.* **1992**, 92, 325–362.
- (21) Fletcher, D. A.; McMeeking, R. F.; Parkin, D. J. *Chem. Inf. Comput. Sci.* **1996**, 36, 746–759 (The UK Chemical Database Service: CSD version 745.738, updated May 2017)..
- (22) (a) Boyd, C. L.; Clot, E.; Guiducci, A. E.; Mountford, P. *Organometallics* **2005**, 24, 2347–2367. (b) Boyd, C. L.; Guiducci, A. E.; Dubberley, S. R.; Tyrrell, B. R.; Mountford, P. *J. Chem. Soc., Dalton*

- Trans.* **2002**, 4175–4184. (c) Guiducci, A. E.; Boyd, C. L.; Clot, E.; Mountford, P. *Dalton Trans.* **2009**, 5960–5979. (d) Guiducci, A. E.; Boyd, C. L.; Mountford, P. *Organometallics* **2006**, 25, 1167–1187. (e) Guiducci, A. E.; Cowley, A. R.; Skinner, M. E. G.; Mountford, P. *J. Chem. Soc., Dalton Trans.* **2001**, 1392–1934.
- (23) Tiong, P. J.; Nova, A.; Groom, L. R.; Schwarz, A. D.; Selby, J. D.; Schofield, A. D.; Clot, E.; Mountford, P. *Organometallics* **2011**, 30, 1182–1201.
- (24) (a) Li, Y.; Shi, Y.; Odom, A. L. *J. Am. Chem. Soc.* **2004**, 126, 1794–1803. (b) Clulow, A. J.; Selby, J. D.; Cushion, M. G.; Schwarz, A. D.; Mountford, P. *Inorg. Chem.* **2008**, 47, 12049–12062.
- (25) Vale, M. G.; Schrock, R. R. *Inorg. Chem.* **1993**, 32, 2767–2772.
- (26) Dreher, A.; Mersmann, K.; Nather, C.; Ivanovic-Burmazovic, I.; van Eldik, R.; Tuzcek, F. *Inorg. Chem.* **2009**, 48, 2078–2093.
- (27) Stout, G. H.; Jensen, L. H. *X-Ray Structure Determination*, 2nd ed.; John Wiley & Sons: Toronto, 1989.
- (28) (a) Latham, I. A.; Leigh, G. J.; Huttner, G.; Jibril, I. J. *Chem. Soc., Dalton Trans.* **1986**, 385–391. (b) Hemmer, R.; Thewalt, U.; Hughes, D. L.; Leigh, G. J.; Walker, D. G. *J. Organomet. Chem.* **1987**, 323, C29–C32. (c) Hughes, D. L.; Leigh, G. J.; Walker, D. G. *J. Chem. Soc., Dalton Trans.* **1989**, 1413–1416. (d) Hughes, D. L.; Jimenez-Tenorio, M.; Leigh, G. J.; Walker, D. G. *J. Chem. Soc., Dalton Trans.* **1989**, 2389–2395. (e) Goetze, B.; Knizek, J.; Noth, H.; Schnick, W. *Eur. J. Inorg. Chem.* **2000**, 2000, 1849–1854. (f) Lehn, J.-S. M.; Hoffman, D. M. *Inorg. Chim. Acta* **2003**, 345, 327–332. (g) Pietryga, J. M.; Jones, J. N.; Macdonald, C. L. B.; Moore, J. A.; Cowley, A. H. *Polyhedron* **2006**, 25, 259–265. (h) Weitershaus, K.; Fillol, J. L.; Wadepohl, H.; Gade, L. H. *Organometallics* **2009**, 28, 4747–4757. (i) Selby, J. D.; Feliz, M.; Schwarz, A. D.; Clot, E.; Mountford, P. *Organometallics* **2011**, 30, 2295–2307.
- (29) Janssen, T.; Severin, R.; Diekmann, M.; Friedemann, M.; Haase, D.; Saak, W.; Doye, S.; Beckhaus, R. *Organometallics* **2010**, 29, 1806–1817.
- (30) (a) Komorowski, L.; Meller, A.; Niedenzu, K. *Inorg. Chem.* **1990**, 29, 538–541. (b) Barrett, A. G. M.; Crimmin, M. R.; Hill, M. S.; Hitchcock, P. B.; Procopiou, P. A. *Organometallics* **2007**, 26, 4076–4079.
- (31) (a) Danopoulos, A. A.; Redshaw, C.; Vaniche, A.; Wilkinson, G.; Hussain-Bates, B.; Hursthouse, M. B. *Polyhedron* **1993**, 12, 1061–1071. (b) Weber, K.; Korn, K.; Schorm, A.; Kipke, J.; Lemke, M.; Khvorost, A.; Harms, K.; Sundermeyer, J. *Z. Anorg. Allg. Chem.* **2003**, 629, 744–754. (c) Fryzuk, M. D.; MacKay, B. A.; Johnson, S. A.; Patrick, B. O. *Angew. Chem., Int. Ed.* **2002**, 41, 3709–3712.
- (32) Johnson, H. C.; Hooper, T. N.; Weller, A. S. *Top. Organomet. Chem.* **2015**, 49, 153–220.
- (33) Pangborn, A. B.; Giardello, M. A.; Grubbs, R. H.; Rosen, R. K.; Timmers, F. J. *Organometallics* **1996**, 15, 1518–1520.
- (34) Fuller, A.-M.; Hughes, D. L.; Lancaster, S. J.; White, C. M. *Organometallics* **2010**, 29, 2194–2197.
- (35) (a) Otwinowski, Z.; Minor, W. *Processing of X-ray Diffraction Data Collected in Oscillation Mode*; Academic press: New York, 1997. (b) *CrysAlisPro*; Agilent Technologies: Oxford, U.K., 2011.
- (36) Altomare, A.; Cascarano, G.; Giacovazzo, G.; Guagliardi, A.; Burla, M. C.; Polidori, G.; Camalli, M. *J. Appl. Crystallogr.* **1994**, 27, 435–435.
- (37) Palatinus, L.; Chapuis, G. *J. Appl. Crystallogr.* **2007**, 40, 786–790.
- (38) Betteridge, P. W.; Cooper, J. R.; Cooper, R. I.; Prout, K.; Watkin, D. J. *J. Appl. Crystallogr.* **2003**, 36, 1487–1487.
- (39) Frisch, M. J.; Trucks, G. W.; Schlegel, H. B.; Scuseria, G. E.; Robb, M. A.; Cheeseman, J. R.; Scalmani, G.; Barone, V.; Mennucci, B.; Petersson, G. A.; Nakatsuji, H.; Caricato, M.; Li, X.; Hratchian, H. P.; Izmaylov, A. F.; Bloino, J.; Zheng, G.; Sonnenberg, J. L.; Hada, M.; Ehara, M.; Toyota, K.; Fukuda, R.; Hasegawa, J.; Ishida, M.; Nakajima, T.; Honda, Y.; Kitao, O.; Nakai, H.; Vreven, T.; Montgomery, J. A., Jr.; Peralta, J. E.; Ogliaro, F.; Bearpark, M. J.; Heyd, J.; Brothers, E. N.; Kudin, K. N.; Staroverov, V. N.; Kobayashi, R.; Normand, J.; Raghavachari, K.; Rendell, A. P.; Burant, J. C.; Iyengar, S. S.; Tomasi, J.; Cossi, M.; Rega, N.; Millam, N. J.; Klene, M.; Knox, J. E.;
- Cross, J. B.; Bakken, V.; Adamo, C.; Jaramillo, J.; Gomperts, R.; Stratmann, R. E.; Yazyev, O.; Austin, A. J.; Cammi, R.; Pomelli, C.; Ochterski, J. W.; Martin, R. L.; Morokuma, K.; Zakrzewski, V. G.; Voth, G. A.; Salvador, P.; Dannenberg, J. J.; Dapprich, S.; Daniels, A. D.; Farkas, Ö.; Foresman, J. B.; Ortiz, J. V.; Cioslowski, J.; Fox, D. J. *Gaussian 09, Revision D.01*; Gaussian, Inc.: Wallingford, CT, USA, 2009.
- (40) Andrae, D.; Haussermann, U.; Dolg, M.; Stoll, H.; Preuss, H. *Theor. Chim. Acta* **1990**, 77, 123–141.
- (41) Ehlers, A. W.; Bohme, M.; Dapprich, S.; Gobbi, A.; Hollwarth, A.; Jonas, V.; Kohler, K. F.; Stegmann, R.; Veldkamp, A.; Frenking, G. *Chem. Phys. Lett.* **1993**, 208, 111–114.
- (42) Weigend, F.; Ahlrichs, R. *Phys. Chem. Chem. Phys.* **2005**, 7, 3297–3305.
- (43) Grimme, S.; Antony, J.; Ehrlich, S.; Krieg, H. *J. Chem. Phys.* **2010**, 132, 154104–154119.
- (44) (a) Lee, A. M.; Handy, N. C.; Colwell, S. M. *J. Chem. Phys.* **1995**, 103, 10095–10109. (b) Ditchfield, R. J. *J. Chem. Phys.* **1972**, 56, 5688–5691.
- (45) Jensen, F. *J. Chem. Theory Comput.* **2015**, 11, 132–138.